The origin of bedrock depression wetlands in the southern Cape of South Africa: a changing perspective

A thesis submitted in fulfilment of the requirements for the degree of

Master of Science

At

Rhodes University

by

Steven Ellery

Supervisor: Fred Ellery

Co-supervisor: John Dunlevey

Abstract

The predominant theory of the origin of depression wetlands in southern Africa was developed by Goudie and Thomas (1985) and focuses primarily on mechanisms relating to deflation and erosion as the main drivers of wetland formation. This theory is based on wind driven deflation of animal watering areas where heavy grazing and trampling of vegetation promotes removal of sediment over short periods of time by wind, to create local depressions and impoundment of water. However, this theory applies in arid and semi-arid areas where grazing can reduce vegetation sufficiently to lead to deflation but does not fully explain the origins of depression wetlands that have formed in moist climates or on ancient erosion surfaces such as the African Erosion Surface (AES). This study investigates the origin of a depression wetland that has formed on sandstone bedrock through weathering and dissolution on the AES in South Africa. Wetlands like this act as groundwater recharge zones such that water flows away from the centre of the depression, taking with it any dissolved solutes derived from weathering of the bed of the depression. Fluctuations between wet and dry periods create both highly reducing conditions (during wet phases) and highly oxidising conditions (during dry phases) beneath the margins of these depression wetlands. Some of the main constituents of the sandstone in this wetland are iron(III) oxides, which are highly sensitive to redox conditions and have therefore been transported to and trapped in the margins of the depression. The redistribution of iron(III) oxides from the centre towards the margins of the depression has caused a net volume loss in the centre of the depression, causing sagging, and a net volume gain at the margins of the depression associated with swelling. This process occurs over periods upwards of a million years and explains the presence of depression wetlands in moist climates.

Acknowledgements

The completion of this Master's thesis would not have been possible without the contributions of many individuals and organisations who have provided superb insight, technical support, emotional support and encouragement throughout the time it took to write this thesis. I would like to extend my gratitude and sincere appreciation to the following organisations and individuals who made this research possible:

- To the NRF who funded parts of this project and continue to support a growing community of researchers in South Africa
- To the iThemba Labs in Cape Town for the XRD analysis and to Remy Bucher for his patience and time that he spent answering the many questions I had for him about XRD analysis
- To the ICP-MS Laboratory in Stellenbosch and to Mareli Grobbelaar for the wonderfully comprehensive and coherent XRF analysis
- To Dr Brigette Melly, Dr Denise Schael, Dr Phumelele Gama and Japie Buckle for taking me to Shadow Vlei and other depression wetlands in the Algoa Bay area – this study would not have been possible without your help and insight – thank you all.
- To my co-supervisor John Dunlevey – thank you for your input. Your constructive critique really changed the way that I thought about the processes of chemical weathering and ferrolysis.
- To Dr Harilaos Tsikos in Geology – thank you for our extremely insightful discussions. Your critical comments and helpful suggestions really revolutionised the way that I thought about iron-cycling and Shadow Vlei in general.
- A massive thank you to all my friends (basically my family) who have provided me with endless encouragement, support, emotional and physical sustenance and for your constant belief in me – you all know how much you mean to me: Robyn, Julián, Jade, J.C., Gina, Geoff, Caitlin, Joana, Dave, Shadow, Shimri, Siya and Katlego.

- To my mother and brother, Karen and Miles, thank you for your unwavering support throughout this thesis. It is an incredible feeling to always know that you have a safe, loving space to go to when the going gets tough.

- And lastly to my supervisor - my father. Dad, your patience and kindness are unmatched, and I could not have asked for a more thoughtful and empathetic supervisor. Thank you for embarking on this adventure with me and for the long hours that we have worked together - patiently and thoroughly thinking about Shadow Vlei. Thank you for all you have taught me – both within and without the bounds of this thesis.

Table of Contents

List of figures

List of tables

List of equations

1 Introduction

Fresh and clean water is becoming an increasingly rare commodity as humans continue to destroy and alter natural systems such as wetlands, rivers and naturally occurring pans and lakes that transport, hold and purify water. It is for this reason, among others, that understanding how these systems function naturally is of utmost importance to the wellbeing of humans and the planet itself. Wetlands form a critical component of the Earth's water resources as they are vitally important features in natural settings and provide many ecosystem services to humans as well (Dugan, 1993). However, wetlands have only been recognised as significant ecosystems in the second half of the 20th century and are therefore still poorly understood from some perspectives. One such perspective that has long been overlooked by wetland scientists is the role of geomorphology in the formation, evolution and perpetuation of wetland systems (Tooth and McCarthy, 2007). Without an understanding of the geomorphological and geological controls that govern the origin, structure, function and dynamics of wetlands and other water bodies, their potential conservation and rehabilitation may be poorly focussed and incomplete. The integration of knowledge about the governing biophysical, hydrological and edaphic processes with the knowledge of governing geomorphological processes of wetlands, will give scientists a much greater depth of understanding of the origin, structure, functioning and dynamics of a given wetland (Ellery *et al.*, 2011). Thus, it is crucial that individuals or groups responsible for managing or rehabilitating these important aquatic ecosystems are informed from an interdisciplinary point of view.

Depression wetlands are a common wetland type that exist across the globe and are found across a wide range of landscapes and climates (Detenback, 2002). These systems are often ephemeral and are characterised by periods of inundation and desiccation and can dry completely during dry seasons. Depression wetlands can be unrecognisable during these periods of desiccation and are often degraded or destroyed because of poor understanding of their origin, structure, function and dynamics (Bowen *et al.*, 2010). They are generally located in localised topographic depressions where surface water accumulates due to precipitation and local runoff, which collects in the depression (Detenbeck, 2002). Water leaving depression wetlands infrequently occurs as surface outflow and is generally removed by evaporation, transpiration or groundwater recharge, meaning that they often occur in dry areas where mean annual evaporation exceeds mean annual precipitation (MAP). However, despite the seasonal nature of most depression wetlands, they are often recognisable as wetlands by their typical wetland vegetation and soil type (Detenback, 2002).

The term depression wetland can be broadly applied to many ephemeral and endorheic water bodies such as pans, playas, dune slacks or depression lakes and is often used interchangeably with these terms. A cause for the confusion in the nomenclature of depression wetlands is due to the poor understanding of their geomorphic origin, structure and function. For the purpose of consistency, the term 'depression wetland' will be used in this thesis to describe endorheic depressions that are characteristically ephemeral and contain typical wetland flora and edaphic features. This study will focus on the geomorphic nature of the formation and evolution of a single depression wetland on the African Erosion Surface (AES) in South Africa, in an attempt to better understand how these systems are formed and therefore how they may be better conserved in the future.

The predominant model that describes the formation of depression wetlands in arid and semi-arid environments was developed by Goudie and Thomas (1985). This model for wetland formation is centred around the process of sediment removal by aeolian means and subsequent deflation of the land surface to form a depression able to hold water (Goudie and Thomas, 1985). This process of wetland formation generally occurs in places where MAP is frequently less than 500 mm and vegetation cover is sparse such that sediment can easily be removed by wind. Aeolian deflation will also not predominate to such great extents in areas where there are highly resistant strata close to the land surface – as is the case on parts of the AES. Therefore, the depression wetland formation theory presented by Goudie and Thomas (1985) can only fully explain the presence of ephemeral depression wetlands in arid or semi-arid areas like the Northern Province, the western parts of the Free State province, parts of Botswana and areas in Namibia where there are lithologies that are susceptible to aeolian deflation as well.

However, depression wetlands occur widely in southern Africa and are commonly found in areas where the MAP is greater than 500 mm, suggesting that the model of wetland formation described by Goudie and Thomas (1985) cannot fully explain their occurrence. For example, there are large depression wetlands widely distributed in the Mpumalanga Province in the northeast of South Africa where MAP is greater than 800 mm. There are also large numbers of depression wetlands that have formed on the AES, often on material that is highly resistant to erosion and weathering. In the Nelson Mandela Bay Municipality alone (ca. 1960 km^2), there are approximately 1700 documented ephemeral depression wetlands, many of which occur on resistant lithologies on the AES or Post Africa I (Melly *et al*,. 2017). The origin of these depression wetlands on the AES cannot be explained using the model presented by Goudie and Thomas (1985). Therefore, the distribution of wetlands across a wide range of climatic conditions as well as a wide range of

lithologies, presents a new area for research in understanding the geomorphic origins of depression wetlands, as well as reconsidering and standardising the nomenclature of depression wetlands.

Recent research has been conducted on depression wetlands that lie on the AES in areas that receive a MAP of more than 600 mm (Alistoun, 2014; Edwards *et al*,. 2016). This research has culminated in the proposal of a new suite of depression wetland origin models that can explain the formation of wetlands on the AES in moist environments through geomorphic processes. The process of long term chemical weathering of bedrock beneath depression wetlands was documented in both Alistoun (2014) and Edwards *et al.* (2016) and can be considered an integral process to the formation of these wetlands. Edwards *et al.* (2016) documented the chemical weathering of a bedrock dolerite sill beneath a wetland, which resulted in a sagging of the earth's surface via localized solute removal, creating a depression able to hold water. A similar sagging effect was documented by Alistoun (2014) whereby bedrock composed of dwyka tillite was chemically weathered. In the case of Alistoun (2014), the presence of broad leaved, woody tree species on the margins of the depression led to ground water movement from the centre of the depression towards its margins as the trees transpired ground water and created a hydraulic gradient away from the wetland centre. The chemical weathering and dissolution of more soluble minerals by water resulted in the lateral transport of solutes towards the wetland margin. Selective uptake of solutes by plants in the margins caused many of these dissolved solutes to precipitate from solution, resulting in a volume expansion and aggradation in the wetland margin and contributing to the formation of a water-holding depression. This work is integral to forming a new suite of depression wetland origin theories that can better explain the wide distribution of depression wetlands in southern Africa.

There may be more pieces to this suite of depression wetland origin theories and that is where the focus of this study lies. In both Alistoun (2014) and Edwards *et al.* (2016), the mineralogy of the bedrock beneath the wetlands was complex such that as chemical weathering progressed, a loss of volume from the parent material was observed. However, if the bedrock beneath a depression wetland is composed of something very resistant and with a very simple mineralogy like quartzitic sandstone, this sagging effect will not be as marked. There are number of depression wetlands on the Southern Cape Coast, westwards of Port Elizabeth, that occur on quartzitic sandstone bedrock (Maud, 2008) in an area that receives more than 600 mm of rain a year (O'Connor and Crow, 1999), which means that neither the depression wetland origin theories presented in Goudie and Thomas (1985) or Alistoun (2014) or Edwards *et al.* (2016) can fully explain their presence. This study aims to address this gap in our knowledge.

2 Aims and objectives

The aim of this study was to examine the geomorphic processes responsible for the formation of Shadow Vlei, situated on the AES north west of Port Elizabeth, South Africa.

To achieve this aim, the following objectives were set:

1. To determine the changes in mineralogical and geochemical composition of the soil at different depths across the centre, the margins and the surrounding areas of Shadow Vlei.
2. To map the topography of Shadow Vlei and surrounding areas.
3. To link patterns observed in the mineralogy and geochemistry to the morphology of Shadow Vlei.
4. To determine the nature of the interaction between the surface water and the ground water in Shadow Vlei.
5. To present a conceptual model of the origin and evolution of Shadow Vlei and to integrate it into the existing origin models for wetlands on the AES in moist environments.

3 Literature review

3.1 The importance of geomorphology in wetlands

The geomorphology of wetlands and the role that geomorphology plays in the origin, structure, functioning and dynamics of wetlands has consistently been overlooked by most wetland scientists. Wetland science has traditionally been the domain of biologists, ecologists and hydrologists and this is reflected in the seminal book *Wetlands* by Mitsch and Gosselink (2015), which is currently in its fifth edition. The model of wetland structure and function that is presented in *Wetlands* and adapted in Figure 1, is the standard model in the field, and emphasises the role of hydrology as the primary driver of the origin, structure, function and dynamics of these ecosystems. The shallow flooding of wetland soils leads to anaerobic conditions in the root zone, which leads to radical changes in soil biogeochemistry, including increased solubility of metals and reduced rates of microbial breakdown of organic matter. These changes in soil biogeochemistry create stressful conditions for life such that only organisms adapted to the absence of oxygen in the root zone, can survive. However, and as can be seen from Figure 1, 'basin geomorphology' and 'climate' are viewed as external factors that broadly affect wetland ecosystems.

The active role that geomorphology plays in shaping wetlands is poorly understood both in Mitsch and Gosselink's (2015) book as well as the many peer reviewed journal articles that are published each year on wetlands. The predominant perception that has been created in the wetland scientific community is that wetland structure and functioning are primarily governed by hydrological, edaphic and biotic factors, and that the geomorphic and climatic setting of the wetland is simply a template upon which these factors act and evolve. This may partly be a consequence of the nature of the work of geomorphologists, which considers processes across a large temporal scale, which seems to be considered irrelevant to understanding wetland structure and function. However, the geomorphology of a wetland is always affecting the way in which a wetland functions and should never be overlooked as a potential source of information about a wetland or as a potential driver of contemporary change within a wetland system (McCarthy and Hancox, 2000; Tooth and McCarthy, 2007). While the contributions of biologists, ecologists and hydrologists are of great significance and have critically aided our understanding, conservation, management and restoration of wetland systems, our practice in wetlands will be far more sustainable if their geomorphology is understood to a similar extent (Ellery *et al.,* 2011). Knowledge of wetland geomorphology will significantly improve our understanding of: 1) wetland origin, dynamics and

evolution; 2) rates of change in wetland form and structure; 3) wetland sensitivity to environmental perturbations and change and 4) likely future trajectories of change in wetland structure and functioning (Tooth and McCarthy, 2007). It is thus argued that the role of geomorphology is brought to the forefront of wetland sciences as it is problematic that our current and predominant understanding of wetlands is based primarily in the fields of biology and hydrology.

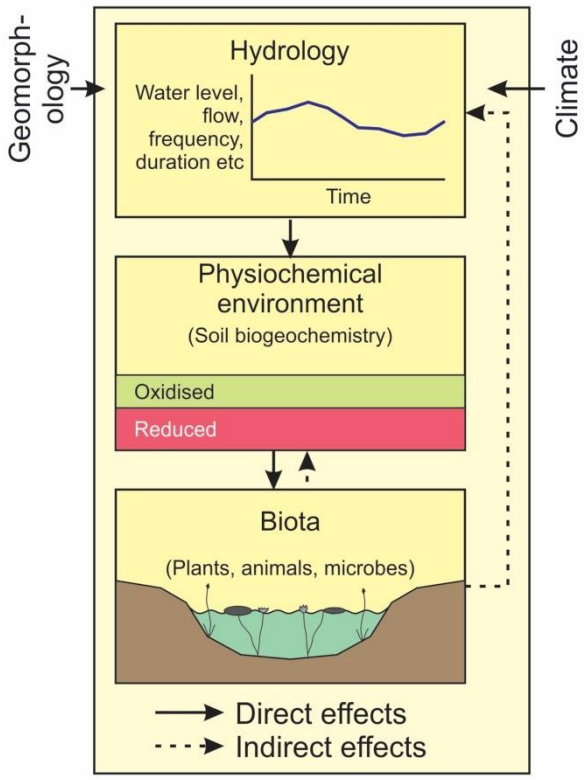

Figure 1: Conceptual model that illustrates the role of hydrology in wetland structure and functioning (adapted from Mitsch and Gosselink, 2015).

3.2 Current models of depression wetland formation

Current understanding of how endorheic depression wetlands are formed is based on a model that was first conceptualised by Goudie and Thomas (1985) for depressions that occur in semi-arid and arid environments. This model primarily considers the role of water and biota and only makes brief mention of the role of geomorphology in the formation of depression wetlands. Central to the model of depression wetland formation presented by these authors is the process of aeolian sediment removal causing deflation. This occurs when surface water collects and stands in an initially small depression on the land surface, typically after a rainfall event. This can often lead to the concentration of herbivores around this water body for the time during which surface water is

present. Localized overgrazing of the vegetation surrounding this feature can thus occur, and in semi-arid areas where mean annual precipitation (MAP) is typically less than 500 mm per annum, this process often leaves the land surface highly susceptible to deflation by wind (Goudie and Thomas, 1985). As these depressions are endorheic, there is little fluvial infilling that takes place such that once the process of deflation has begun, the net sediment budget of the depression is negative. This model developed by Goudie and Thomas (1985) was further refined by Thomas (2011), who identified three suites of controls that either work individually or in combination with one another to form depression wetlands.

Structural Controls: Structural controls refer to the ways in which the geology and the geomorphology of a given area will have a potential effect on the formation of depression wetlands. Faulting, rock fracturing and warping of the earth's crust can influence the drainage patterns and the ways that groundwater interacts with surface water. These controls influence the direction of groundwater flow and drainage patterns of a given catchment and can therefore potentially affect depression wetland genesis. These structural controls are often responsible for the initiation of depression wetland formation, after which other controls might become the dominant mechanism for wetland formation and evolution (Thomas, 2011)

Ponding Controls: Ponding controls refer to processes whereby flow of water on the land surface is interrupted by an obstruction, leading to a ponding effect. Examples of this can be found in linear depressions that occur between dunes in a dune field or when sedimentation of abandoned river beds causes back-ponding and depression wetland formation. The obstruction of water flow in valley or floodplain wetlands by large sedimentary deposits such as tributary alluvial fans also cause a ponding effect that may result in the formation of a depression wetland (Grenfell *et al.*, 2009).

Erosional Controls: Erosional controls refer to the processes described in Goudie and Thomas (1985) whereby wetlands are formed through the process of deflation because of overgrazing around localized depressions in areas with low MAP. The erosional controls are influenced by climatic controls such as rainfall, temperature and seasonality, as well as biotic controls such as the presence/absence of herbivores and vegetation structure and composition. If the depression initiation site is situated on lithologies that are susceptible to erosion and the areas surrounding the depression have low average slope gradients, there will be no fluvial integration and hence a lack of fluvial sediment transport into or out of the depression. These factors work in combination with the biotic and climatic

controls and result in a negative sediment budget for the wetland initiation site and hence a depression wetland will begin to form.

The current understanding of the formation of these depressions is based on research that was conducted almost exclusively in semi-arid and arid areas where MAP is generally less than 500 mm. The model proposed by Goudie and Thomas (1985) therefore does not explain the presence of pans in wetter climates where MAP is greater than 500 mm and deflation because of overgrazing is unlikely as vegetation cover is persistent despite heavy grazing. Most of the research on depression wetland formation also only considers wetlands that have formed on lithologies that are not highly resistant to erosion, even though there are many documented cases of depression wetlands having formed on highly resistant strata. However, in recent years there has been research conducted that has looked at the formation of depression wetlands occurring in much wetter climates and on resistant lithologies, and a new suite of depression wetland formation models have been proposed through this research (Alistoun, 2014; Edwards *et al.,* 2016).

3.3 Surface sagging associated with deep weathering

In work done by Edwards *et al.* (2016) on a wetland on the Karkloof Plateau in the KwaZulu-Natal Midlands, where MAP is 870 mm, another set of processes that resulted in the formation of a depression in which peat accumulated were documented. The wetland is called Dartmoor Vlei and it sits upon a large bedrock dolerite sill that has been extensively intruded by several dolerite dykes – one of which is situated at the toe of the wetland (Figure 2A) and acts as a local base level for the Dartmoor Vlei (ibid). The dolerite sill upon which the vlei sits is on the African Erosion Surface and is resistant to weathering and erosion. Weathering of this sill is therefore likely to be extremely slow. Permanent hydration of the bedrock dolerite sill means that it has undergone a process of prolonged chemical weathering that is associated with mineralogical simplification as well as the loss of metals, particularly iron. Weathering of Dartmoor Vlei is thought to have begun in the early Cretaceous period and solutes lost from the parent bedrock during weathering were removed from the system via groundwater recharge and possibly via surface outflow (ibid). As the chemical weathering process took place, 'sagging' occurred whereby the surface of the wetland sank to an elevation lower than the dolerite dyke at the toe of the wetland. Calculated volume losses amount to about 3 %, which means sagging of between 8 and 9 % given that the volume loss is only expressed vertically. Given weathering to a depth of almost 10 m, the volume loss of the dolerite sill amounted to sagging by about 1 m (Figure 2C). This sagging process has resulted in the lowering of the overall slope of the Dartmoor Vlei and a gradual decrease in the ability of the

wetland to carry clastic sediment because flow throughout the wetland is diffuse. The prolonged weathering of the dolerite sill and sagging of the wetland surface has caused a ponding effect within the wetland as the dolerite dyke at the toe of the wetland now acts both as a local base level as well as a natural impoundment (Figure 2C, ibid). This ponding effect has resulted in the formation of a depression wetland that is not strictly endorheic in nature.

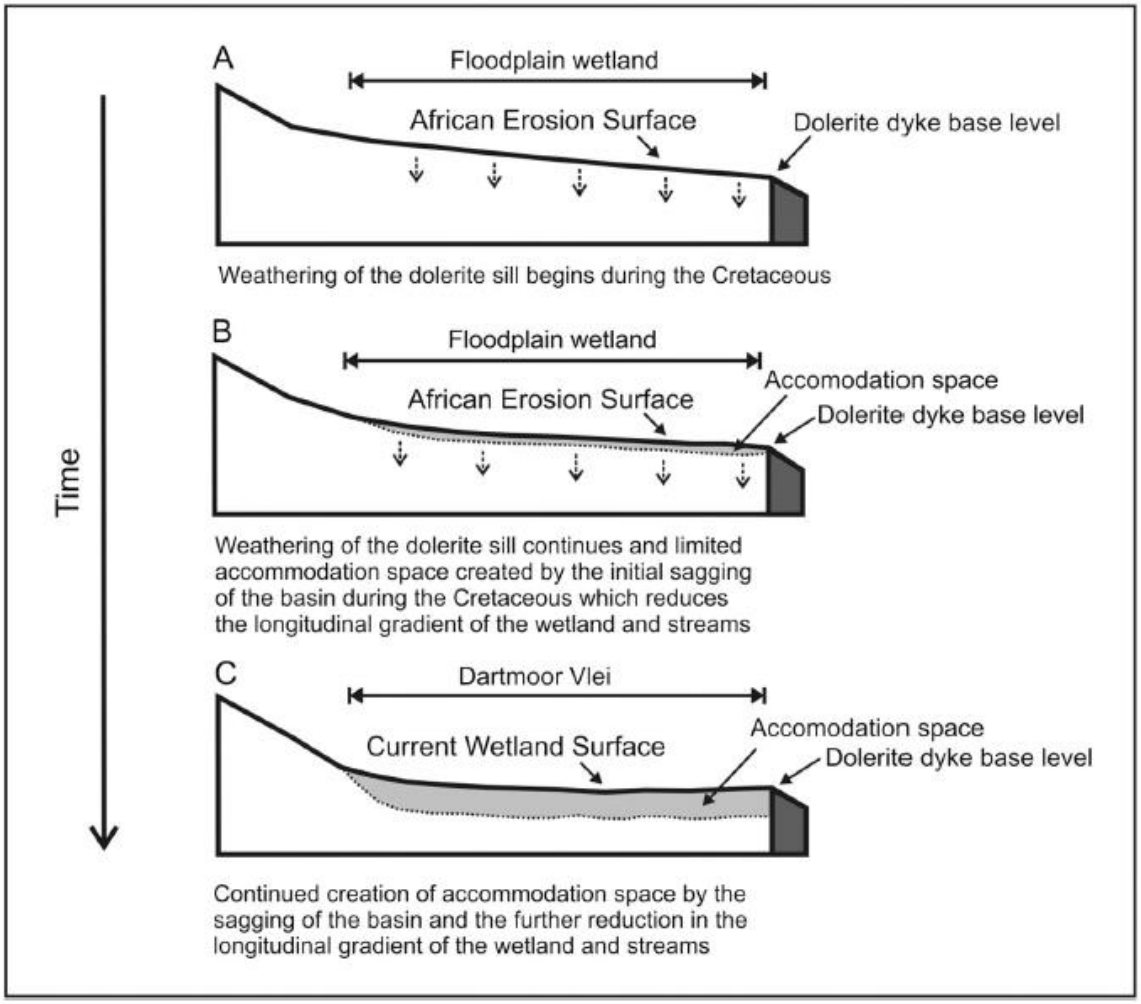

Figure 2: A conceptual model of the origin and evolution of Dartmoor Vlei (adapted from Edwards *et al.* 2016).

3.4 Aggradation through evapotranspiration and solute precipitation: Lessons from the Okavango Delta

The processes contributing to the formation of islands in the Okavango Delta have been studied extensively (McCarthy *et al.*, 1993; Ellery *et al.*, 1993; McCarthy and Ellery, 1994; McCarthy and Ellery, 1998) as the Delta, situated in Northern Botswana, is southern Africa's largest wetland with a surface area of approximately 18 000 km^2. The delta is in fact a large alluvial fan with a very low gradient (ca. 1:3400) with two distinct physiographic parts; the upper linear panhandle section and the lower delta shaped alluvial fan region. The lower alluvial fan section of the Okavango Delta is dotted with islands of varying size, with similar patterns of vegetation composition and zonation (Ellery *et al.*, 1993; Smith, 1976). The margins of these islands are raised above the centre of the island and are often populated with dense stands of evergreen, broad leaved trees and shrubs, while the centres of the islands are characterised by sparse grass cover, and are sometimes devoid of vegetation (Figure 3). The structure and composition of the vegetation on these islands plays an integral role in their formation and evolution.

McCarthy *et al.* (1993) found that the water table beneath these islands is lower than that of the surrounding swamps as a result of the presence of these broad leaved evergreen trees in the island margin and the fact that they have their roots in the water table and transpire large quantities of water into the atmosphere (Figure 3). Transpirational water loss in the island fringe leads to lowering of the water table and to the creation of a hydraulic head from the swamp to the centre of the island (McCarthy *et al.*, 1993). This hydraulic head induces ground water movement towards the centre of the islands, bringing with it dissolved solutes. Trees growing in the island margin are selective in their uptake of solutes such that many solutes that are limiting to plant growth are excluded. This leads to an increase in electrical conductivity from the swamp water surrounding each island towards the centre of the island. The electrical conductivity of the waters in the Okavango Delta, particularly of groundwater beneath islands, is related to the evapotranspirational water loss from the ecosystem, such that as water is lost to the atmosphere, electrical conductivity increases. Sodium remains in solution throughout the evapotranspirational process and precipitates from solution at the end of the process of water loss to the atmosphere (Ellery *et al.,* 1998; Figure 4a). This means that sodium is conserved during evapotranspirational water loss as it will remain in solution until the last bit of solvent is evaporated, which typically happens at the centre of the island at the soil surface, where it forms a white efflorescent crust that is toxic to

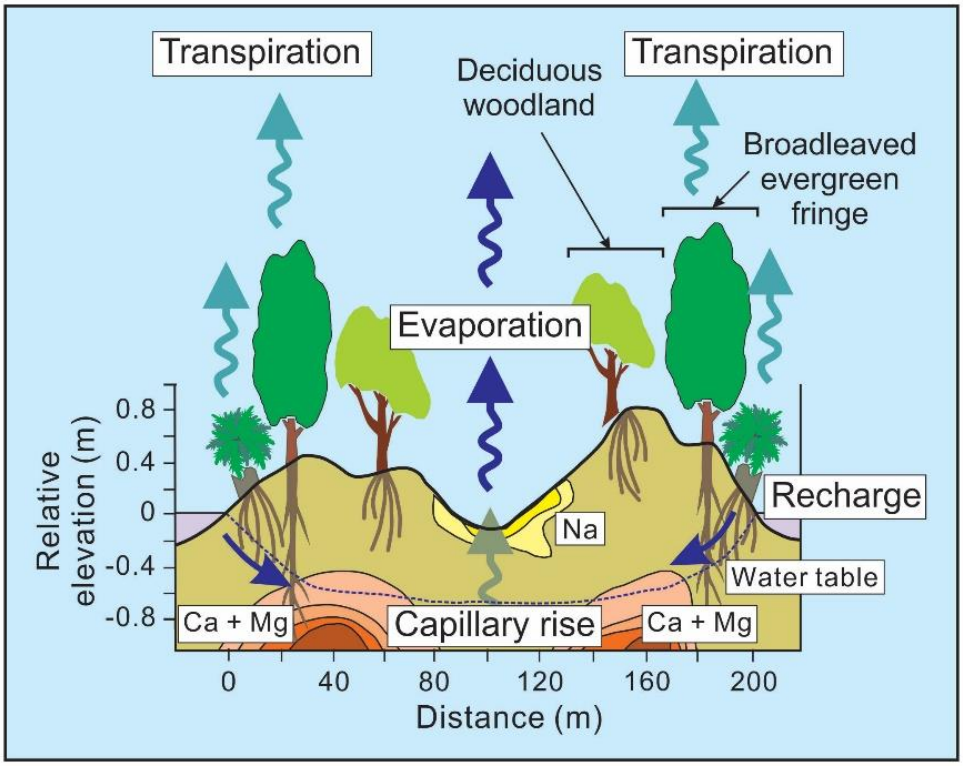

Figure 3: Summary diagram of the most important processes through which water moves below ground and is lost from islands in the Okavango Delta (adapted from Ellery *et al.,* 1998).

vegetation. The same is not true for other dissolved solutes such as calcium or silica. At relatively low concentrations of sodium, the concentration of calcium increases in proportion to the concentration of total dissolved solutes due to transpiration and evaporation. However, at a concentrations of 100 ppm Ca, the concentration of calcium decreases as the electrical conductivity continues to increase due to transpirational water loss (Figure 4b; McCarthy *et al.,* 1993). This means that as transpirational water loss continues to increase the concentrations of other solutes, calcium is no longer conserved in solution and precipitates from solution as calcium carbonate ($CaCO_3$). The precipitation of calcium in the soil near the island margin causes the soil to swell, leading to the creation of topographic relief in the island margin and the formation of a depression in the centre of the island.

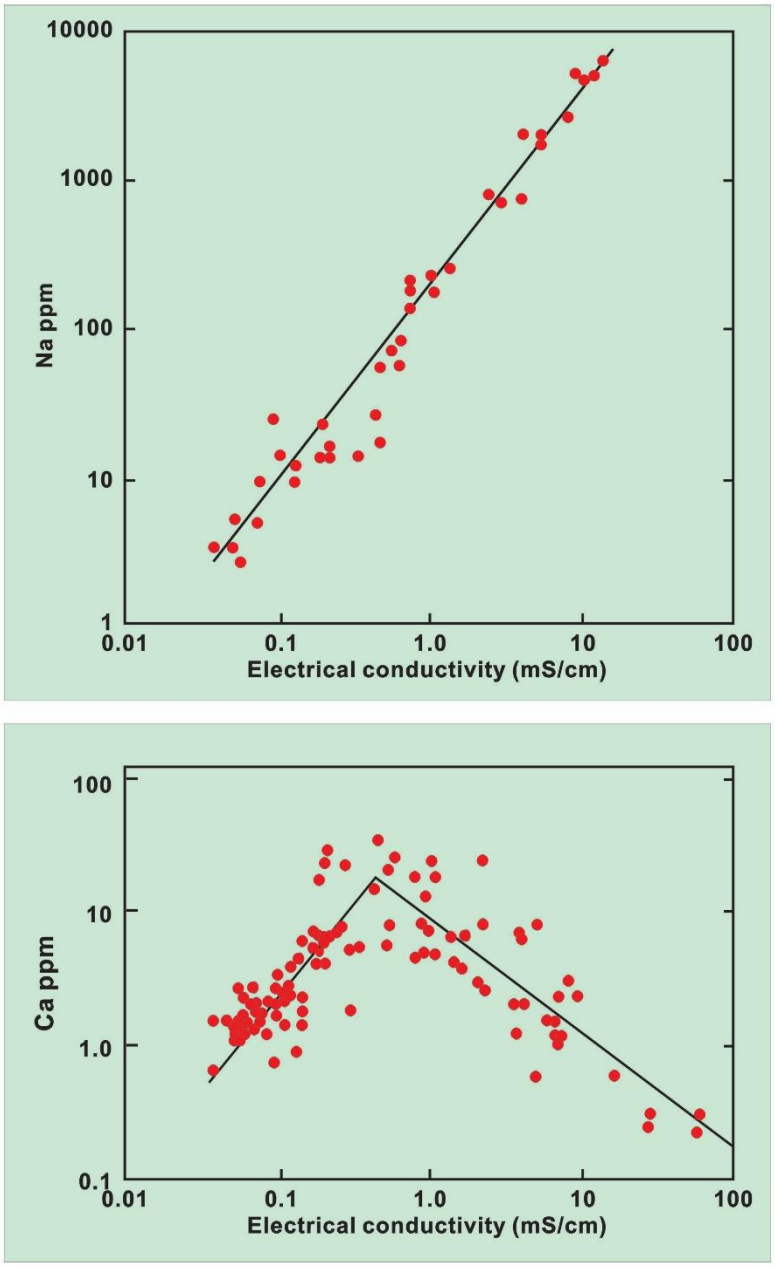

Figure 4: Plot of sodium (a) and calcium (b) concentrations in relation to electrical conductivity for surface and ground water samples in the Okavango Delta (McCarthy *et al.,* 1993).

3.5 Wetland formation through sagging of a central depression and aggradation of the depression margin

Alistoun (2014) documented another suite of processes that led to the formation of a depression wetland through a combination of sagging and aggradation. The wetland that was examined is situated on commonage land north of Grahamstown on the African Erosion Surface, where the MAP is 680 mm (Sinchembe and Ellery, 2010). It is situated within the Albany thicket biome which

is comprised mainly of evergreen *Sclerophyllous* species mixed with many succulent shrub species (Cowling, 1983). The vegetation composition on the fringe of the wetland is dominated by large woody species that have large and deep root systems that are responsible for the uptake of groundwater from the water table. The depression wetland itself sits upon weathered bedrock of dwyka tillite and acts as a groundwater recharge zone whereby the water surface in the wetland is elevated in comparison to the water table on the margin of the wetland. This elevated water surface in the wetland creates a hydraulic head that slopes away from the depression and sustains the recharge of groundwater away from the depression to the surrounding areas.

After rainfall events, any local depression, even small ones of limited depth, will fill with water and lead to localized hydration of the soil (Figure 5a). Such hydration, particularly under anaerobic conditions, accelerates dissolution of mineral phases which are lost to the groundwater (Figure 5b). The hydration of the bedrock and associated chemical weathering leads to mineralogical simplification and loss of mass and volume as described for Edwards *et al.* (2016; Figure 5c). Because the wetland acts as a groundwater recharge zone, there will be lateral movement of groundwater away from the depression towards the margins, where deep-rooted evergreen trees have their roots in the water table. This outward movement of water transports dissolved solutes leading to solute removal from the centre of the wetland that is responsible for the sagging experienced there.

Due to the selective uptake of water by trees and the exclusion of solutes, the solute load in groundwater increases to a point where dissolved solutes precipitate from solution in the fringes of the depression, causing aggradation of the margins (as documented by Ellery *et al.,* 1993). The lateral removal of chemical constituents from the centre of the depression causes sagging, while solutes thus generated, most notably calcium and magnesium, are precipitated in the margins of the depression, causing the soil to swell and leading to aggradation (see Figure 5d). It is unlikely that the processes documented by Alistoun (2014) and Edwards *et al.* (2016) would occur in semi-arid or arid areas where prolonged hydration and chemical weathering of the bedrock is unlikely, as is the occurrence of deeply rooted vegetation and the lateral movement of solutes.

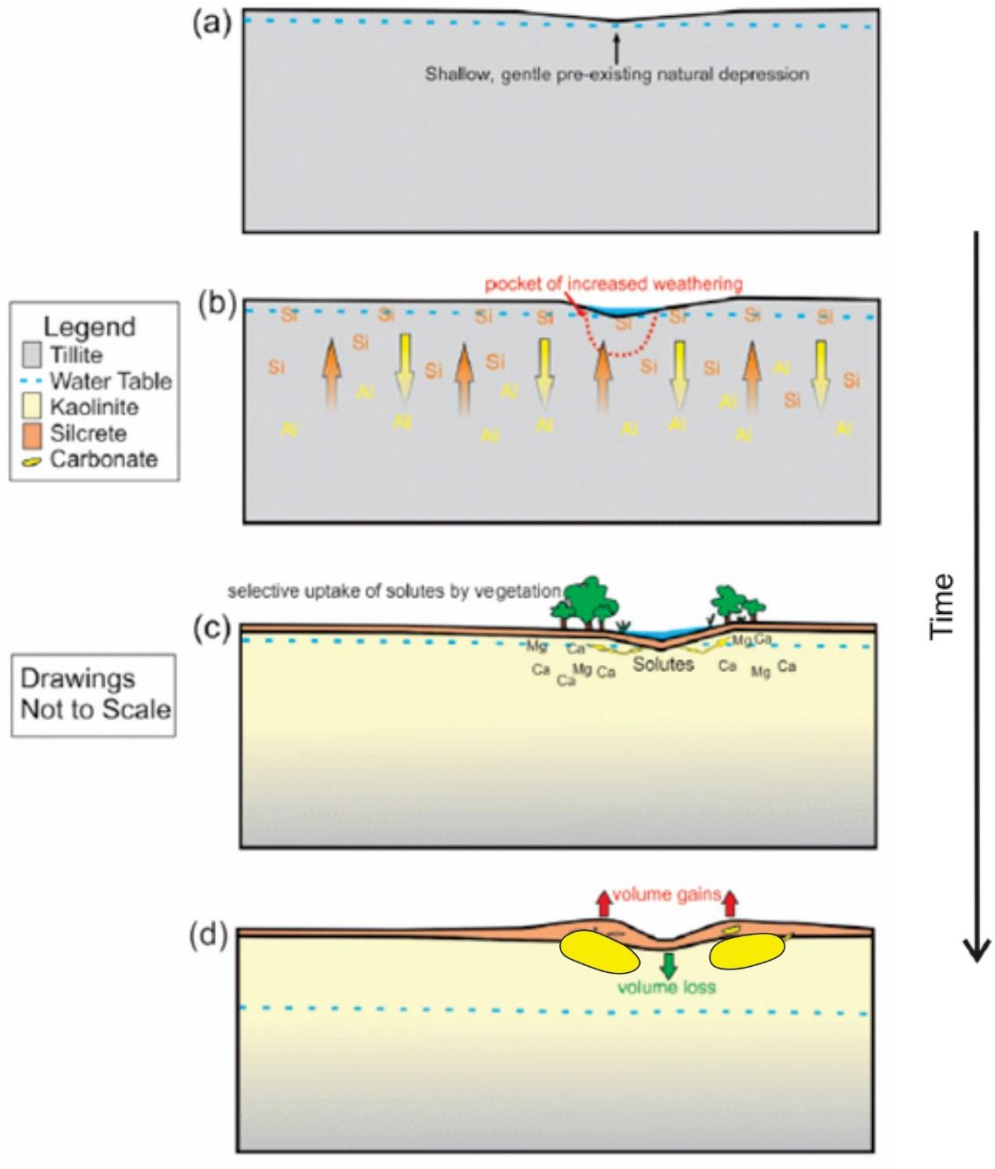

Figure 5: A conceptual model for the formation of a depression wetland on the African Erosion Surface near Grahamstown (adapted from Alistoun 2014).

3.6 Chemical weathering

To fully comprehend the processes of sagging and aggradation that are described in Edwards *et al.* (2016), Alistoun (2014) and Ellery *et al.,* (1993), it is important to understand concepts associated with chemical weathering. Weathering is a term that describes the physical and chemical alteration of minerals or rocks near or at the earth's surface that is caused by chemical factors that interact with climatic factors and biological processes (Birkeland, 1984). For the purposes of this discussion, chemical weathering is the primary process relevant, and further discussion will therefore only deal with this. Chemical weathering involves the attachment or detachment of

atoms from minerals that make up a parent body of rock. The rate and extent of this process is affected by the composition of rock being weathered as well as the external conditions under which weathering is taking place, such as ambient temperature and moisture availability (White and Brantley, 1995).

There are six different ways in which material can be chemically weathered namely; hydration, hydrolysis, dissolution, oxidation-reduction, carbonation and chelation (Krzic, 2004). There are several factors that affect the rate of chemical weathering such as temperature, surface area of saprolite, pH of solvent, atmospheric pressure, oxidation-reduction conditions and the composition of material that is undergoing weathering (Anderson and Anderson, 2010). Chemical weathering takes place at increased rates at higher temperatures and in humid conditions. The composition of the rock undergoing weathering affects the rate of weathering as well. For example, rock with high concentrations of quartz takes much longer to weather than rock made up mainly of clay-forming minerals (White & Brantley, 1995). The larger the surface area of exposed rock being weathered, the faster the weathering process, such that if a rock is fractured into many small pieces, the surface area will be much greater and hence the weathering process will happen faster. Chemical reactivity of a solvent also affects the rate of chemical weathering. For example, if carbon dioxide is dissolved in rainwater to create a weakly acidic solution, it will be far more effective at breaking ionic bonds between minerals than water with a neutral pH (Krzic, 2004).

The alteration of the chemical and physical properties of rock most often occurs in the presence of water as it is a universal solvent and is abundantly available in natural systems. As water permeates through the cracks and pore spaces of rocks, it will react with and dissolve atoms present in the rock. Minerals are made up of a range of elements that vary in their solubility in water (Anderson and Anderson, 2010). For example, Ca^{2+}, Na^{+} and K^{+} are more soluble in water and will go into solution before Al^{3+} and Si. As solutes are dissolved by water, they are moved by groundwater flow to a different location, including the stream network. This process of solute transportation by water is fundamental to the progression of chemical weathering and there are two effects of chemical weathering that are pertinent to this discussion.

The first effect is the alteration of the chemical composition of the mineral that is undergoing weathering. As solutes are preferentially removed from the parent material based on their solubility, the chemical composition of that material will change and a new mineral (or minerals) will be formed (Figure 6). This preferential removal of the most soluble constituents by water is relatively consistent and predictable and is referred to as incongruent dissolution. The dissolution of the potassium feldspar (orthoclase) occurs in the presence of water and is an example of

incongruent dissolution (see Equation 1). The dissolution of orthoclase produces silicic acid ($Si(OH)_4$), potassium ions and a clay mineral called kaolinite ($Al_2Si_2O_5(OH)_4$) which is a common mineral end member of feldspar weathering in natural conditions.

Equation 1: Incongruent dissolution of orthoclase to form kaolinite through dissociation of K^+ ions.

$$2KAlSi_3O_8 + 11H_2O \rightarrow Al_2Si_2O_5(OH)_4 + 4Si(OH)_4 + 2K^+ + 2OH^-$$

In the context of chemical weathering, incongruent dissolution leads to the formation of new minerals. Another example is when a muscovite mica is hydrated, leading to dissolution of the most reactive component, which in this case is K^+. Over time, most of the K^+ ions will be lost from the weathering interface and eventually an aluminium smectite will be formed (see Figure 5). Aluminium smectites comprise minerals that are much more resistant to weathering – mainly aluminium silicate minerals – which take much longer to dissolve in water. Therefore, through elemental simplification, the parent material in a weathering profile will be chemically simplified and become much more resistant to weathering (Anderson and Anderson, 2010).

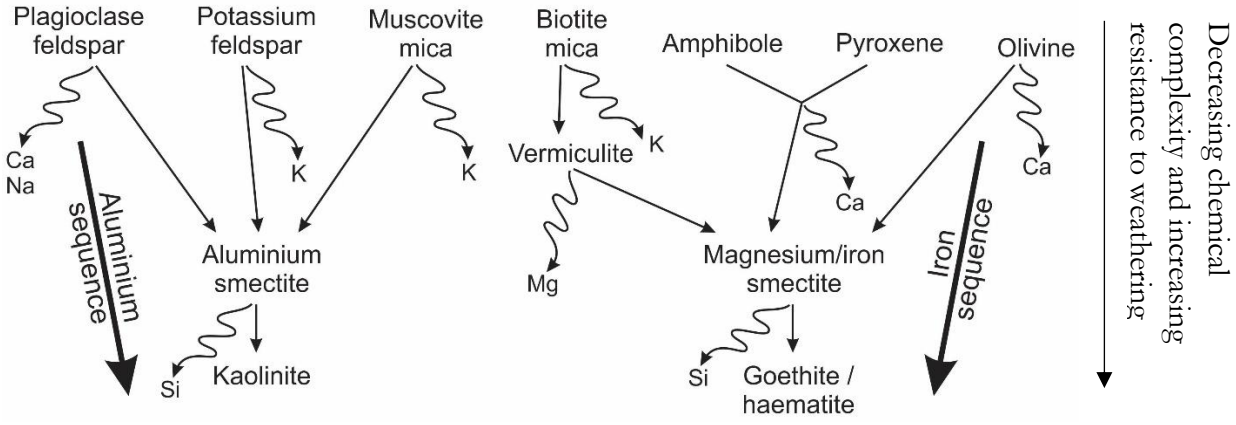

Figure 6: Typical weathering steps of major silicate mineral groups. Primary minerals are displayed across the top. Curved lines represent cations that are lost to solution and straight lines represent changes in mineral state (adapted from Taylor and Eggleton, 2001).

The second effect of chemical weathering is the physical alteration of the parent material. As the parent material is chemically weathered slowly over time and chemical constituents are removed, physical changes to the parent material will also take place. One physical feature that will change is the density of the parent material because of the physical removal of solutes from the weathering interface (Anderson and Anderson, 2010). Some of these physical changes manifest in the form of cracks, fractures and enlarged pore spaces within the weathering rock – all of which are forms

of isovolumetric weathering. Isovolumetric weathering is a form of weathering where there are no observed changes in the volume occupied by the material undergoing weathering (Anderson and Anderson, 2010). However, if chemical weathering persists for long enough, the pore spaces, cracks and fractures will permeate deeper and more abundantly through the body of the rock and will weaken the rock sufficiently for collapse to occur. As a result of such a collapse, a loss in volume and sagging of the land surface will be observed. This process of volume and mass loss is what Edwards *et al.* (2016) and Alistoun (2014) observed in the centres of the depression wetlands that they studied. The loss of volume due to weathering can also be accompanied by a gain in volume in a location where the dissolved solutes from the weathering profile eventually precipitate from solution. A large proportion of dissolved solutes associated with the process of chemical weathering end up in stream systems and eventually in the ocean, but a significant proportion of these dissolved solutes may be transported to other terrestrial locations. Continuous precipitation of solutes in a single location over time can have the opposite effect of chemical weathering and can in turn fill pore spaces and cracks in the rock, and ultimately lead to volume gains (Anderson and Anderson 2010). The precipitation of Ca^{+} and Mg^{+} in the margins of the depression wetland that Alistoun (2014) studied is responsible for aggradation and the gains in volume that were observed in her study.

The weathering processes that result in topographic alteration of the land surface typically take extended periods of time and as the chemical composition of the mineral undergoing the weathering process is simplified, this process will happen at an exponentially reduced rate.

3.7 Contextualizing Shadow Vlei

Shadow Vlei is a depression wetland that is located within the Nelson Mandela Bay Municipality (NMBM) boundary about 30 km north west of Port Elizabeth. Shadow Vlei is one of approximately 1700 small, ephemeral, non-fluvial wetlands that occur in the NMBM (Schael *et al.*, 2015). The approximate density of these wetlands is about nine per 10 km^2, which is a significant number. Melly *et al.* (2017) have worked for several years mapping and explaining the presence of these wetlands in the NMBM from both biological and geomorphic points of view and have made great progress towards a more holistic understanding of their existence in this area. This project will hopefully supplement their growing understanding of wetlands within NMBM. Due to the relatively large range of climates, lithologies and geomorphic settings across which these wetlands occur, it is unlikely that they all share a common origin. It may be the case that several of the wetlands located in the low rainfall zones of the NMBM are formed primarily by wind driven

deflation. However, wetlands that occur within wetter areas of the NMBM and on resistant lithologies such as the Table Mountain Group or the Uitenhage sandstones cannot be explained by the Goudie and Thomas (1985) model of wetland formation because many of them are on bedrock.

Shadow Vlei occurs on the Table Mountain Group sandstones and is in the wetter parts of the NMBM. According to Melly *et al.* (2017), this depression, and many others like it, is formed because of the presence of a perched water table. A perched water table is created by a hard, semi-impermeable layer that lies below the surface of the ground and has limited connectivity with the regional water table. The presence of an aquitard beneath a precipitation-fed endorheic wetland will encourage lateral flow of groundwater as opposed to vertical flow – much like the process described in both Alistoun (2014) and Ellery *et al.* (1993). There are a variety of aquitards that were identified by Melly *et al.* (2017) that include bedrock perches, bedrock and clay perches, clay perches and calcrete perches. The origin of these perches was not explored in either Schael *et al.* (2015) or Melly *et al.* (2017), but Shadow Vlei was assessed in both studies and the presence of a bedrock and clay perched water table was confirmed.

Another significant feature of Shadow Vlei that was noted upon initial inspection is the presence of large exposed ferricrete deposits that surround the central depression and form part of a raised marginal area. Ferricrete is an iron-rich sedimentary rock that is characterised by ferruginous and siliceous conglomerates and clasts that are cemented together in an iron and aluminium sesquioxide rich matrix (Widdowson, 2007). Ferricretes are some of the most abundantly occurring duricrusts in terrestrial environments and are often found in depositional features at the toe of hillslopes or in localised depressions. Characteristic of ferricrete profiles is the allochthonous nature of the materials that solidify to form a ferricrete duricrust – which distinguishes ferricretes from laterites, which are autochthonous iron rich duricrusts (Widdowson, 2003). The formation of ferricrete requires input of allochthonous material that is generally derived from chemical weathering and lateral transportation of solutes by water (Widdowson, 2007). Iron, which is one of the primary constituents of ferricrete, is often liberated from a weathering front during the break-down of silicate minerals and is released as ferrous iron (Fe^{2+}; Equation 2), which is easily oxidised to ferric iron (Fe^{3+}; Equation 3) in the presence of oxygen, typically forming the mineral goethite or hematite.

Equation 2: Dissolution of fayalite in the presence of carbonic acid to form ferrous iron in solution, bicarbonate and silicic acid.

$$Fe_2SiO_4 + 4H_2CO_3 \rightarrow 2Fe^{2+} + 4HCO_3^- + H_4SiO_4$$

Equation 3: Reduction of ferrous iron in an oxygen rich zone below ground to form insoluble ferric iron and carbonic acid.

$$4Fe^{2+} + O_2 + 8HCO_3^- + 4H_2O \rightarrow 2Fe_2O_3 + 8H_2CO_3$$

Ferric iron is extremely insoluble and often becomes fixed in the soil profile as clasts or conglomerates which can eventually coalesce and form a cement that binds siliceous and aluminous clasts together to form ferricrete. However, ferric iron can be reduced in anaerobic conditions in the presence of soil microbes, as microbes are known to reduce minerals that contain oxygen in their lattice structure (Mitsch & Gosselink, 2015). Anaerobic conditions are often created naturally below ground when there is saturation by water after a rainfall event. Anaerobic conditions in combination with microbial activity and fluctuating pH levels are also conducive for the weathering of siliceous minerals such as feldspars or micas, and therefore it is common to see the removal of silicon from the zone where the water table exists. Because iron is sensitive to both reducing and oxidising conditions that occur in the zone of a fluctuating water table, iron is often trapped and enriched in this zone (Figure 7; Widdowson, 2007). Thus, ferricrete is often formed as a consequence of prolonged interaction with a fluctuating water table and is often characterised by a zone where iron is enriched, and silicon is depleted.

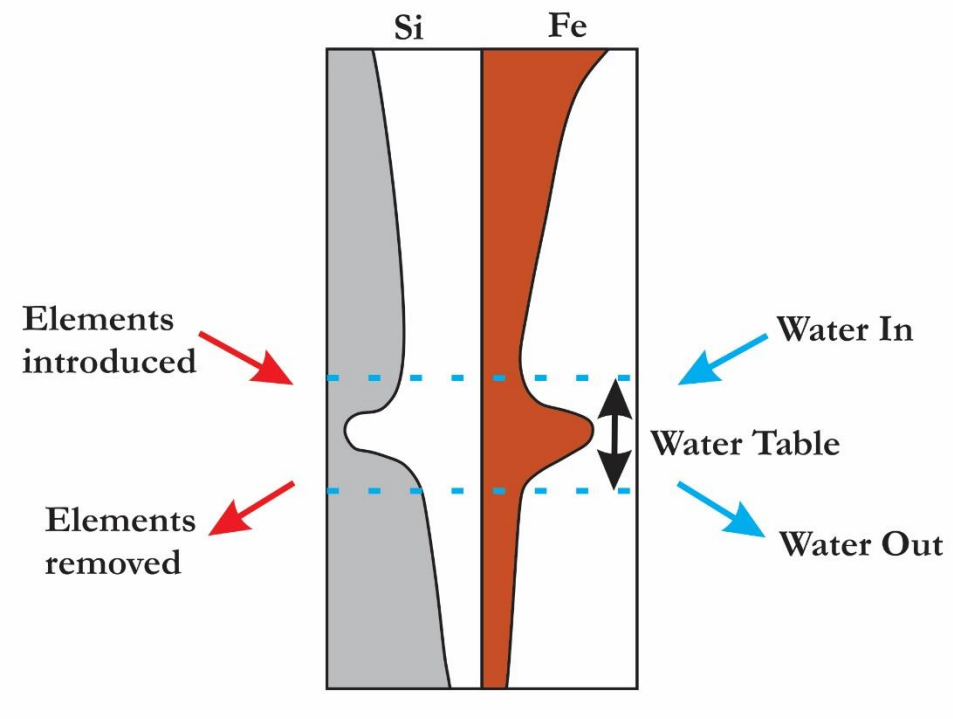

Figure 7: Schematic representation of changes in silicon and iron abundances in a typical ferricrete alteration profile (adapted from Widdowson, 2007).

Ferricrete and the movement of iron appear to play an important role in the formation of Shadow Vlei as the raised margins are widely populated with ferricrete duricrusts. Several attempts to auger in the margins of Shadow Vlei were confounded by the widespread presence of large iron and silica rich clasts and conglomerates – which are indicative of newly forming ferricrete below ground.

4 Study Area

Shadow Vlei (Figure 8) is situated on commonage that borders the northern fence of the Hopewell Estate Nature Reserve, which is approximately 30 km North West of the centre of Port Elizabeth. Shadow Vlei is one of four ephemeral depression wetlands that are situated in very close proximity to one another, two of which are within the borders of the Hopewell Estate Nature Reserve. Shadow Vlei is 230 m above sea level and is located at 33°52'20"S and 25°24'38"E.

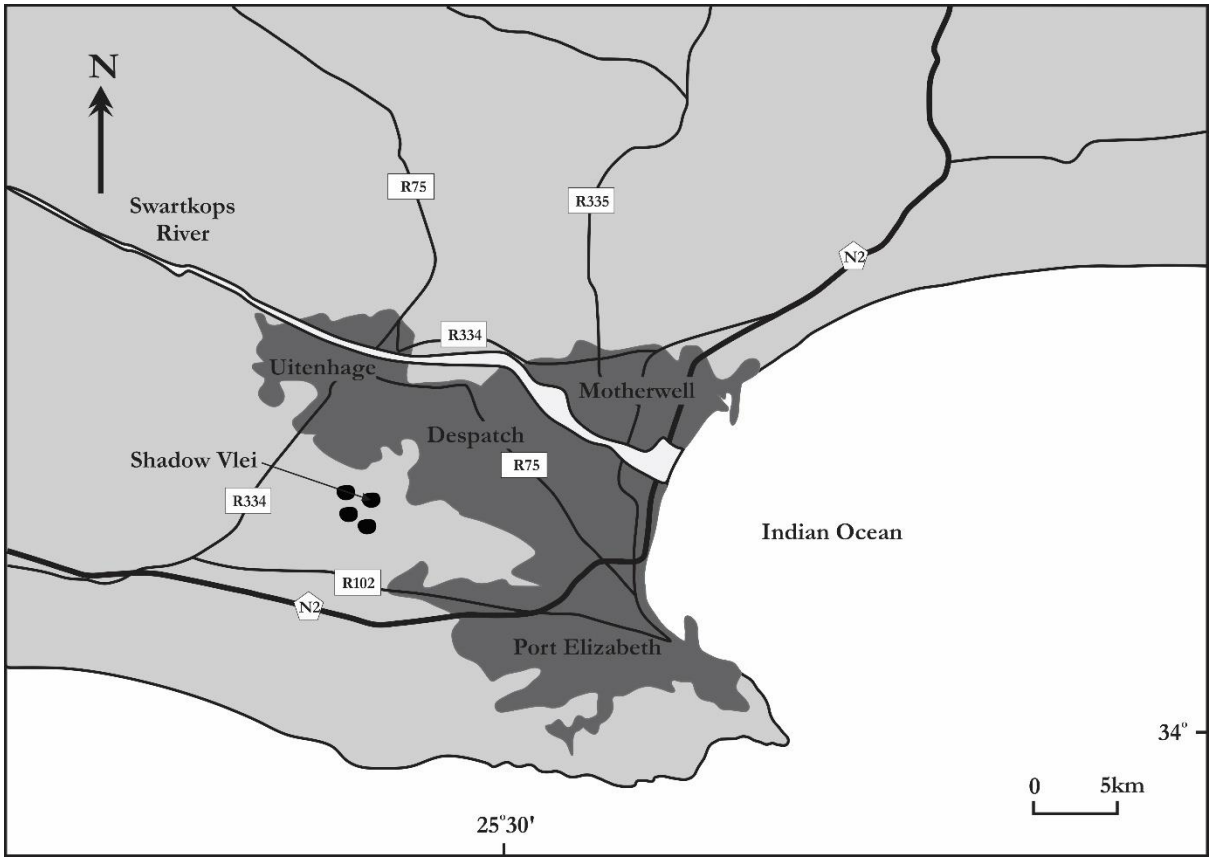

Figure 8: Map of the location of Shadow Vlei. Size of depression wetlands not drawn to scale.

4.1 Climate

The climate of Port Elizabeth and the surrounding areas is warm and temperate, receiving between 500 mm and 850 mm of rain a year (Mucina and Rutherford, 2006). This rainfall occurs throughout the year because Port Elizabeth and the wider Algoa Bay area receive both summer and winter rainfall. During the winter months, the coastal regions of South Africa receive frontal rainfall from the easterly movement of mid-latitude low pressure cells off the south coast of the country. The

rainfall associated with these mid-latitude low pressure cells is predominantly light because these low pressure cells lose energy as they progress from the Western Cape in an easterly direction (Singleton and Reason, 2007). Precipitation in Port Elizabeth during the spring and early summer months is a consequence of cut-off low systems. Cut-off low systems are created when a low-pressure system is 'cut off' from the larger planetary circulation systems and can become stagnant or very slow moving. The slow moving nature of cut-off low systems means that they can bring intense and prolonged rainfall events that can cause significant flooding (Jacobs, 2017).

The average daytime temperature of Port Elizabeth and surrounding areas is 16 °C while the average night-time temperatures is 12 °C (O'Connor and Crow, 1999). The warmest months in this area are January and February which have mean temperatures of 20 °C and the coldest month of the year is July which has an average temperature of 14 °C (O'Connor and Crow, 1999). Temperatures can regularly rise above 30 °C in January and February and seldom drop below 10 °C in the winter months. The climate in the Algoa Bay area is not conducive to the formation of frost and an average of three frost days are experienced a year (Mucina and Rutherford, 2006). However, the mean annual evaporation for Port Elizabeth and the surrounding areas is 1500 mm and can sometimes reach up to 3000 mm in extreme years (Midgeley *et al.*, 1994).

4.2 Geology, soils and geomorphology

Shadow Vlei lies upon the African erosion surface (AES) which is an ancient surface that was formed over a long period of time, starting with the breakup of Gondwanaland in the early Cretaceous some 140 Ma (Partridge and Maud, 1987). The AES is a gently undulating to flat surface and is the product of long periods of weathering and erosion – hence the name 'erosion surface'. The AES was shaped and formed over a period of 120 million years (although most of its formation occurred in the first 20 million years after Gondwanaland broke up) until the subcontinent of southern Africa experienced two epeirogenic uplift events approximately 20 Ma and 5 Ma (Partridge and Maud, 1987). The first uplift event caused the eastern coast and eastern interior of southern Africa to rise 200-300 m and the western coast to rise approximately 150 m – resulting in a gently downward sloping interior from east to west. The second uplift event resulted in an 800 m rise in the east and a 100 m rise in the western parts of southern Africa, further exacerbating the westward tilting interior. Each uplift event is characterized by a new erosion surface which are known as Post Africa I and Post Africa II erosion surfaces. Erosion surfaces form due to lowering of stream base levels following uplift, which leads to downcutting, which is followed by lateral erosion of incised valleys (Anderson and Anderson 2010). Over the period

between the Miocene and Pleistocene (~20 Ma to present), much of the original AES has eroded away and there are not many well-preserved portions of the AES left.

It can be difficult to decipher the difference between the AES and the Post Africa I and II erosion surfaces, especially in areas towards the coast where uplift events were not as pronounced and the vertical distinction between the erosion surfaces is not always clear. Partridge and Maud (1987) mapped the erosion surfaces and according to their macro-scale map depicted in Figure 9, Shadow Vlei lies on a partly planed section of the AES to the west of Port Elizabeth. In many areas the AES is characterized by the presence of silcrete, which is the product of long term weathering and dissolution of silica in warm moist conditions experienced during the Cretaceous period (Maud, 2008). However, the climate dried and cooled at the end of the Cretaceous and much of the silica that had been weathered during the Cretaceous was concentrated near the surface of soil profiles and solidified into silcrete duricrusts or silcrete nodules (Maud, 2008). On the AES, these silcrete nodules are often cemented together by siliceous or ferruginous cements – both of which are found in abundance in Shadow Vlei.

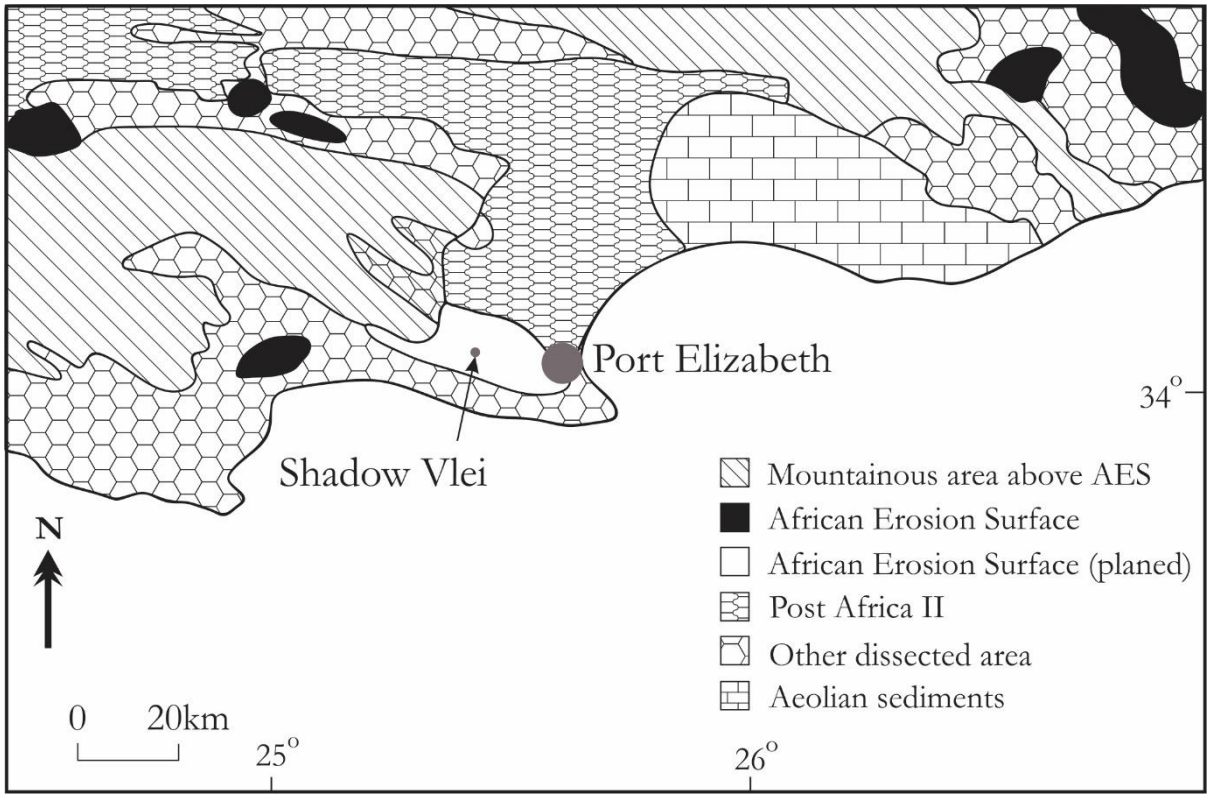

Figure 9: Location of Shadow Vlei in relation to the African and Post-African erosion surfaces (adapted from Partridge and Maud, 1987).

The AES is characterized by many different lithologies, but Shadow Vlei is located on the eastern most stretch of the Cape Subfacies B Table Mountain Group sandstone (Visser, 1974). In the area south of Uitenhage, the Table Mountain Group conformably overlies 500 m of grey quarzitic sandstones and shales and is approximately 2500 m thick itself (Visser, 1974). The sandstone upon which Shadow Vlei lies is composed primarily of mature quartz arenite within a feldspathic sandstone matrix – although the feldspars don't normally amount to more than 5 % of the total mineralogy (Visser, 1974). The surface of the lithology contains traces of iron and aluminium and therefore appears to be a brick red colour on the surface. However, due to the extent of weathering within the Cape Subfacies B Group, the lithology gets lighter with depth and an almost white colour is observed at a depth of more than 5 m.

The predominant soil type in which Shadow Vlei is located is the hard-eluvic Wasbank soil form (Soil Classification Working Group, 1991). Wasbank soils are grouped into plinthic soils characterized by enriched iron oxide concentrations and often occur in areas where a fluctuating water table gives rise to both aerobic and anaerobic conditions below ground (Fey, 2010). The fluctuation of the water table gives rise to the reduction and mobilisation of iron below ground as well as its reprecipitation as mottles, nodules, concretions and hardpan (such as ferricrete). Plinthosols are widely distributed in South Africa but are seldom found in regions of extremely low or extremely high rainfall (Fey, 2010). Plinthic soils and the iron rich concretions that characterise them are often formed via iron enrichment from allochthonous sources and generally occur at the bottom of hillslopes or depressions where periodic wetting and drying of the soil is common. The Wasbank soil form is characterised by a surficial orthic A horizon that is dark brown to grey in colour and is extremely hard when dry (Soil Classification Working Group, 1991). An E horizon occurs below the orthic A horizon in Shadow Vlei, the E horizon being a lighter brown/grey colour as a consequence of a fluctuating water table and iron removal. The E horizon consists of 6-15 % clay minerals and overlies a hard plinthic B horizon which is characterised by an indurated zone of iron oxide accumulation. The hard plinthic B horizon is characterised by extensive iron concretions and ironpan formations and is extremely hard – requiring a percussive drill to break through it.

4.3 Vegetation

The vegetation found in this area belongs to the Humansdorp Shale Renosterveld vegetation type which is often found on argillaceous sedimentary lithologies like shales, and have been documented on sandstone and mudstone lithologies as well (Mucina and Rutherford, 2006). Shale

Renosterveld is the most widely occurring renosterveld group as it accounts for 86 % of the total renosterveld vegetation type. Renosterveld is often characterized by areas where rainfall patterns allow for high grass cover (chiefly *Merxmuella stricta*) and therefore are often affected by local grazing and fire regimes (ibid). Thicket patches are often converted to renosterveld for grazing purposes through controlled burning.

The Humansdorp Shale Renosterveld vegetation type is found along the coastal forelands between Port Elizabeth and Humansdorp and stretches inland to Patensie and Uitenhage and commonly occurs between fynbos and thicket vegetation types in these areas. The coastal forelands are characterized by moderately undulating hills that occur between 20~400 masl and occur in areas where MAP ranges from 500-850 mm (mean: 630 mm; ibid). The vegetation is composed of medium dense graminoid species such as *Themeda triandra, Eustachys paspaloides, Cynodon dactylon* and *Merxmuellera disticha* mixed with dense cupressoid-leaved shrubland species such as *Elytropappus rhinocerotis, Helichrysum anomalum, Oedera genistifolia* and *Anthospermum galioides* (ibid). Thicket and fynbos often occur in small patches in the Humansdorp Shale Renosterveld. This vegetation type is endangered as it is widely used as grazing lands and the three endemic plant species *Delosperma patersoniae, Trichodiadema fourcadei* and *Cyrtanthus wellandii* that exist in this vegetation type are threatened by intense grazing regimes. Only 6 % of the total area covered by the Humansdorp Shale Renosterveld vegetation type falls within conservation areas (ibid).

4.4 Human Land Use

Shadow Vlei lies on a large section of municipal commonage situated between the Hopewell Estate Nature Reserve and the KwaNobuhle Township, which lies approximately 7 km to the north of the wetland. The areas immediately surrounding the northern and north-eastern edges of the commonage are occupied by areas in which people live in low-cost housing. The commonage is utilized extensively by the people from KwaNobuhle for livestock grazing (cattle, goats, sheep), for mining the quartz rich sandstones and for hunting and gathering various natural resources. Several light industrial businesses have their workshops and warehouses along main roads in the area such that there is a fair amount of industrial activity within the vicinity of Shadow Vlei. Approximately 200 m to the south of Shadow Vlei lies the Hopewell Estate Nature Reserve which is a private nature conservation estate. There is a clear distinction between the health of the vegetation in the commonage and that of the vegetation in the Hopewell Estate Nature Reserve as the commonage is used extensively for grazing by local livestock owners. This indicates the

importance of private conservation areas and their ever growing contribution to conserving natural ecosystems in South Africa (Cousins *et al.*, 2008).

5 Methods

5.1 Mapping topography

The topography of Shadow Vlei was measured along eight survey transects that intersected at the centre of the depression. These eight transects started about 100 m outside the depression, passed through the central point and extended about 100 m beyond the opposite margin of Shadow Vlei so that its relief could be contextualised in relation to the surrounding land surface. The survey data was collected using a Topcon GTS 211D total station device and a staff with a reflective prism. The topographic survey included all the points where cores were taken. The absolute position of each survey point was recorded using a handheld Garmin GPSMap 64s GPS. The elevation of the depression was determined by tying the survey data in with a spot height depicted on a topographic map located 50 m north of Shadow Vlei. A contour map of Shadow's pan and the surrounding area was then constructed.

5.2 Sample collection

Samples were extracted from nine cores taken along two perpendicular transects that intersected at a common core at the centre of the depression such that three of the cores were located outside of the depression margin, two were in the depression margin and four were within the depression itself. Coring was undertaken using a 1996 Thor Drilling Rig equipped with a 100mm diameter percussion drill and a 1995 Ingersoll Rand Air Compressor XHP900. In each core, soil samples were collected at depth intervals of 10 cm such that after drilling each 10 cm interval, the air compressor was used to blow the sampled material back up the core hole. This material was caught on a large plastic sheet above ground and stored in a durable brown paper bag. Each core was drilled to a depth of 4 m, while two parent material samples were extracted from a depth of 10 and 11 m.

5.2.1 Sample categorisation based on soil colour

Soil samples were dried at 60 ºC until no further weight loss was measured. About 50 % of the sample was passed through a 1 mm sieve. The colour of each sieved sample was determined by placing material on a blank, clean sheet of A4 paper and photographing it using a Canon IXUS 185 digital camera. The distance between the camera and the soil sample was kept constant using a tripod, and two lamps with white bulbs were set up pointing towards the soil sample to give

blanket white light across the sample. Each photograph was then opened in CorelDRAW x6 and an average cyan, magenta, yellow and key (CMYK) colour code of the soil sample was obtained using the eyedropper tool. The eyedropper tool was set to sample an area of 25 square pixels to generate an average CMYK value for the sampled pixels.

Each soil sample was then categorised into one of eight colour classes derived from a classification of samples based on their average CMYK values. This allowed a colour profile of each core to be constructed. Whenever there was a change in the colour of the soil and a change in colour category, a sample from the middle of the new category was selected for analysis. On this basis 70 samples from the nine cores were selected for X-ray diffraction (XRD) and X-ray fluorescence (XRF) analyses.

5.2.2 Sample preparation for laboratory analysis

The 70 samples selected for chemical and mineralogical analysis were crushed using a Lead Herzog Swing Mill. For these samples material was taken from the bulk sample that had been oven-dried but had not been sieved. Samples generally consisted of both fine particulate matter and larger clast particles, which had to be broken up using a jaw vice before milling process. Each sample was crushed to a fine powder of <75 μm after two minutes in the swing mill. Each soil sample was then split with one half used for an XRF analysis to assess the chemical composition of samples and the other half was used for XRD analysis to assess the mineralogical composition of the samples.

5.2.3 X-ray diffraction analysis

A qualitative XRD analysis was carried out at the iThemba Labs in Cape Town where a D8 Powder X-ray diffractometer system equipped with a theta-theta goniometer was used. Copper radiation (CuKα; $\lambda K\alpha_1$=1.5406 Å) and a 0.034 second step time was used for a continuous XRD scan. The analysis was carried out over a 2θ range of 5-80^o and each XRD pattern produced was analysed using the built in Bruker EVA software in combination with ICDD PDF 1999 database. A total of 70 samples were sent for XRD analysis in labelled glass vials; each sample contained approximately 2 g of crushed material.

XRD analyses are based on the constructive interference between monochromatic X-rays and a given soil sample. Monochromatic X-rays are directed at the sample and the interaction between the incident rays and the sample produce a diffracted X-ray based on the lattice structure of the sample. The diffraction of X-rays is detected after the sample has been rotated through a variety

of orientations relative to the incident X-ray. All possible diffraction directions should be attained and counted due to the random orientation of the powdered material as it is rotated. All the diffraction directions of the lattice structure of the sample can be analysed based on the distribution and size of diffraction peaks. The diffraction peaks can be converted to d-spacings using a known formula and minerals can be identified on a standard d-space reference chart as each mineral phase has a unique set of d-spacings. The d-spacing or the *hkl* Miller indices of a mineral refer to the unique 3D spaces between planes in a crystal lattice structure. The interaction between the monochromatic X-rays and the d-spacing of a given mineral will produce a unique diffraction pattern. Based on the number of times each diffraction peak is observed, an accurate mineralogical composition for each sample can be obtained.

5.2.4 X-ray fluorescence analysis

The quantitative XRF analysis was carried out at Stellenbosch University using a PANalytical Axios Fast WDXRF spectrometer using an Rh tube. The XRF analysis was used to determine the weight percentage of the major elements (Al_2O_3, CaO, Cr_2O_3, Fe_2O_3, K_2O, MgO, MnO, Na_2O, P_2O_5, SiO_2 and TiO_2). The same 70 samples that were sent for XRD analysis were sent for XRF analysis following the same sample preparation as for XRD analyses.

XRF analyses allow for the accurate determination of the chemical composition of a soil sample and they work on the principle of fluorescence. Fluorescence is a process whereby an electron is knocked out of its atomic orbital by another particle (in this case the energy from the x-ray) which is followed by a release of energy specific to the affected element. The energy released is related to the difference in binding energies between the electron orbitals of an element and are referred to the d-spacings of that element. Each element has a unique set of d-spacings (distance between orbitals of an element and not synonymous with the d-spacings ascribed to crystal lattice structures) such that the energy that is released during a fluorescence interaction can be measured and attributed to a specific element. Each time an electron is displaced from a sample during an XRF analysis, the energy that is released because of fluorescence is measured and the elemental composition of a sample can be determined.

5.3 Data Analysis

5.3.1 Mapping the topography

The data collected from the topographic survey was downloaded from the total survey station and was processed using Microsoft Excel. The downloaded data was converted into a series of coordinates and elevations, after which a contour map was sketched on graph paper. A contour interval of 0.5 m was used to construct the map.

5.3.2 XRD data analysis

The qualitative XRD data received from iThemba was initially compiled and analysed in Microsoft Excel. A semi-quantitative analysis was then performed on a select number of samples using the Material Analysis Using Diffraction (MAUD) program. MAUD is a general diffraction/fluorescence/reflectivity program based primarily on the Rietveld method and can be used for quantitative phase analysis (Bish and Howard, 1988). However, there are many problems inherent with the quantitative phase analysis of natural rock samples. There are many variables and steps in the process of XRD analysis that, if not treated with caution, could skew quantitative results. A number of these problems were encountered in attempting to quantify mineralogical composition, but it was generally possible to assign the abundances of phases to within about 15 % of the sample concentration. Nevertheless, there was no attempt made to determine the accuracy of the quantitative abundances of minerals assigned to each sample, which would have been sensible practice. One of the main problems that was encountered during the analysis was that many of the mineral phases present in the samples were poorly crystalline and did not produce sharp, distinctive diffraction peaks. This was further confounded by the fact that the quartz phase present in the sandstone was crystalline and produced very sharp, intense diffraction peaks such that some of the smaller peaks might have been lost in the background noise of the diffraction pattern. Crystallographic analysis of clay minerals is also difficult as clay particles are flat and can give inconsistent diffraction signals based on their orientation at the time of diffraction. Common practice for the quantitative analysis of clay minerals is to separate the clay particles from the rest of the sample via a process of disaggregation or centrifugal separation, and to quantify them separately on a prepared sample mount (Towe, 1974). It was not possible to separate the clay fraction from the bulk sample in this study as this was only considered in retrospect, which meant that only bulk samples were sent for analysis.

The difficulties of quantitative phase analysis were considered at length and attempts were made to account for these inconsistencies in the final presentation of the XRD results. The greatest source of potential error during the MAUD analysis was the difference in crystallinity that exists between quartz and other phases present in each sample. This inconsistency was partially accounted for by interpreting the XRD results in relation to the XRF results. All the most commonly occurring minerals in the sampled material are aluminium-silicates meaning that the ratio of Al_2O_3 : SiO_2 in the XRF data is correlated to the ratio of aluminium-silicates : quartz in the XRD data. The concentrations of aluminium-silicate materials were adjusted using these ratios. The ratios of aluminium-silicate minerals were adjusted in relation to the concentrations of their end-member cations obtained by XRF. Goethite was only detected in the qualitative phase analysis in samples that contained >5 % Fe_2O_3 and thus, concentration of goethite in the semi-quantitative analysis was adjusted according to the ratio of SiO_2 : Fe_2O_3 obtained by XRF.

The semi-quantitative results from the MAUD analysis were initially processed in Microsoft Excel, after which they were analysed using the statistics package R. Descriptive statistics were applied to the mineral dataset for summarizing. Regression and correlation statistics were then derived to determine relationships between mineral distribution and to assess the distribution relationship between the mineral phases and the chemistry of soils.

5.3.3 XRF data analysis

The data that was received from the XRF analysis was analysed using a variety of programs and methods. The initial data processing and statistical analyses were conducted in Microsoft Excel, after which the final statistical analyses and graphs were produced using R. Most of the data analysis focused on establishing relationships between concentrations of SiO_2, Fe_2O_3 and Al_2O_3 because they often accounted for >90 % of the chemical composition of any given sample.

The raw fluorescence data was used to construct six isoline cross-sections that depict the distribution of SiO_2, Fe_2O_3 and Al_2O_3 beneath Shadow Vlei. These cross-sections were initially sketched on graph paper, after which they were digitally reconstructed using CorelDRAW x6. Descriptive statistics were applied to the data set to create a series of boxplots that allowed for the visualization, summary and description of the concentrations and variability of each of the oxides. Regression and correlation statistics were utilized to create scatterplots that were initially used to determine relationships between different oxides in the geochemical dataset.

A hierarchical agglomerative cluster analysis was used to group samples with similar chemical compositions, which allowed for the identification of patterns in the distribution of different

oxides below ground across the length and breadth of the depression. Descriptive statistics were used to determine statistical characteristics of the concentrations of SiO_2, Fe_2O_3 and Al_2O_3 within each cluster. One-way ANOVAs were then used to highlight statistical differences between each cluster. A Tukey's HSD post-hoc test was conducted on the ANOVA results to determine the differences between individual oxide concentrations between clusters. A covariant principal components analysis (PCA) was also run on the entire chemical dataset to determine which oxides were contributing most to the variation within the dataset. The results from the cluster analysis were then superimposed on to the PCA biplot to give better resolution to the scatter of points on the plot itself.

6 Results

6.1 Morphology of Shadow Vlei and surficial ferricrete distribution

The morphology of Shadow Vlei is distinctly atoll shaped, with margins that are raised above a central depression as well as above the land surface that surrounds the depression (Figure 10). The entire wetland is approximately 200 m in length and 120 m in width and the average difference in elevation between the centre and the margins is 3 m. A crescent-shaped mound exists on the north side of the depression where there are large ferricrete outcrops. The eastern margin of Shadow Vlei is almost entirely covered by a large section of ferricrete duricrust with smaller ferricrete outcrops that are scattered around the marginal areas of the wetland (Figure 10). These ferricrete outcrops vary in thickness, but the average thickness of the ferricrete duricrusts is between 1 and 2 m. The average gradient between the centre of the depression and the top most point of the margin is 3.13 % whereas the gradient away from the depression towards the surrounding landscape in any direction is less than 1 %.

6.2 Geochemistry of Shadow Vlei

6.2.1 Variation in chemical composition of soils

6.2.1.1 Description of heterogeneity based on simple statistics

The geochemistry of Shadow Vlei is relatively simple as it is a highly weathered system and most of the soluble chemical constituents have likely been removed from the parent material. The more soluble constituents include CaO, Cr_2O_3, K_2O, MgO, MnO, Na_2O and P_2O_5 which exist only in very small quantities – generally <1 % (Figure 11A). CaO shows the largest variation of all the oxides present in the soil with a minimum concentration of 0.02 % to a maximum concentration of 3.41 %. However, the oxides displayed in Figure 11A do not contribute a large proportion of the overall content of the soil mass, together making up approximately 10 % of the weight of the sample. They are therefore likely to have a negligible effect on the morphology of the depression. Between 2 % and 7 % of the material comprises organic matter, bound water or hydroxyl compounds that together are measured as loss on ignition (LOI). The soil is predominantly composed of Al_2O_3, Fe_2O_3 and SiO_2 with SiO_2 making up the largest proportion of the soil mass with an average concentration of 83.14 %, while Fe_2O_3 and Al_2O_3 are present in similar quantities with average concentrations of 5.26 % and 5.62 % respectively (Figure 11B).

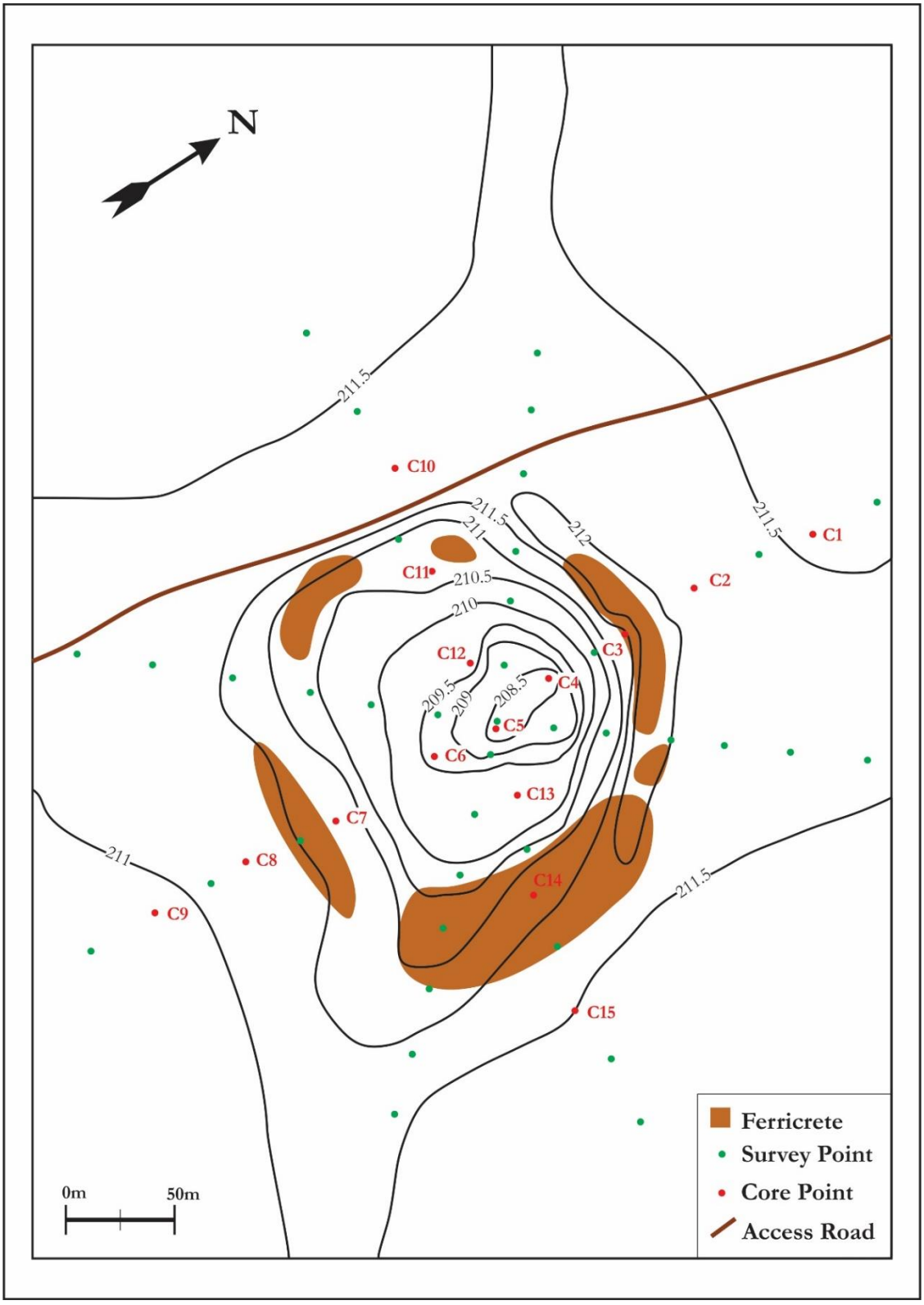

Figure 10: Topography of Shadow Vlei. Contour interval is 0.5 m. The first transect line runs in a north-south direction and the second transect line runs almost perpendicular to the first.

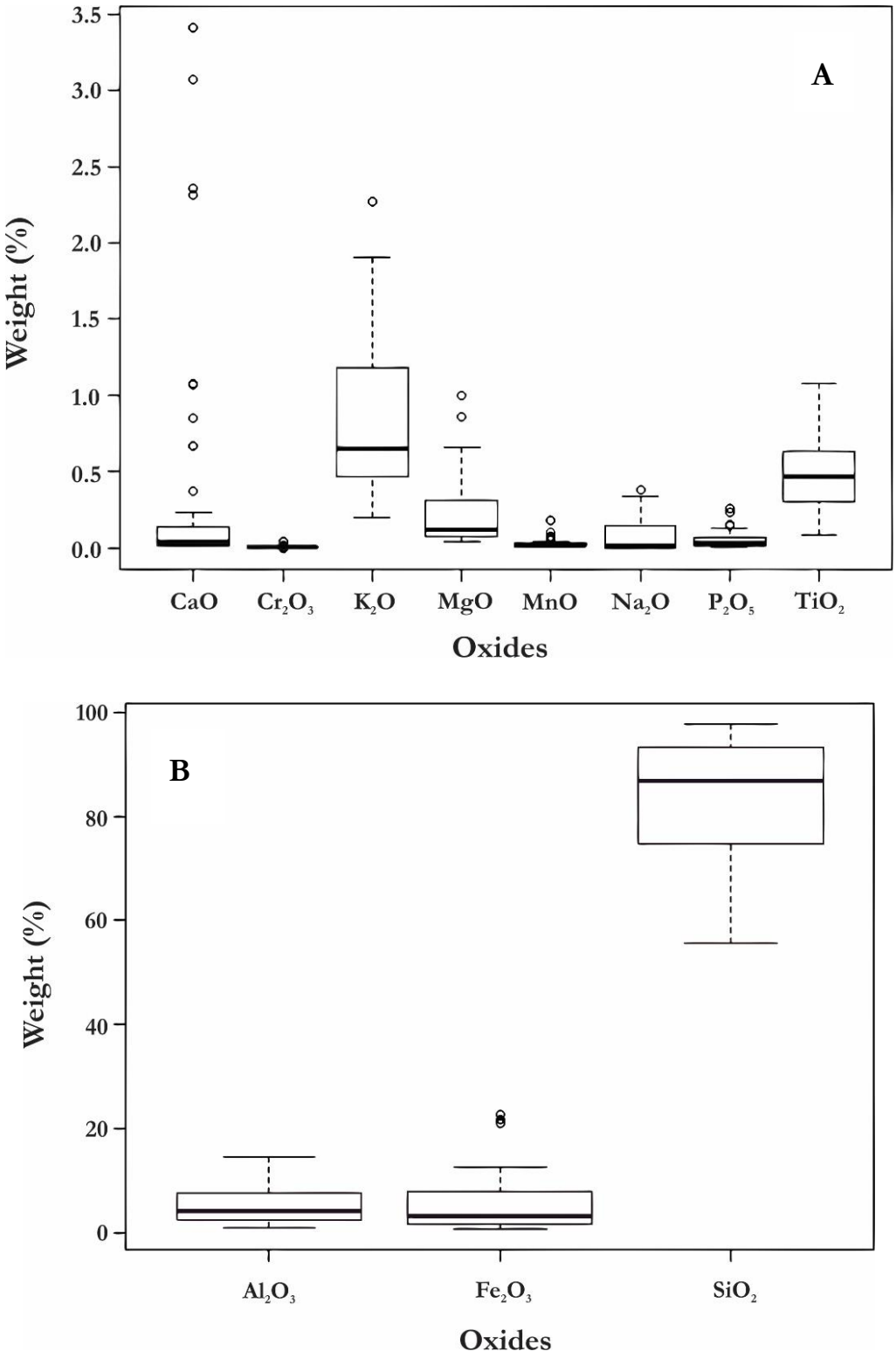

Figure 11: Box and whisker plots of the different minor (A) and major (B) oxides present within the geochemistry of Shadow Vlei. Whiskers show average standard deviation.

Figure 11B shows the variation in the mean weight percentage of SiO_2, Fe_2O_3 and Al_2O_3. SiO_2 has a minimum value of 55.64 % and a maximum value of 97.8 %. Fe_2O_3 has a mean concentration of 5.16 %, a minimum of 0.710 % and a maximum of 22.7 %. Similarly, Al_2O_3 has a mean concentration of 5.61 %, a minimum weight percentage of 0.873 % and a maximum weight percentage of 14.6 %. The geochemistry of Shadow Vlei is therefore comprised primarily of the oxides of these three elements (Si, Al and Fe).

6.2.1.2 Analysis of heterogeneity based on multivariate analysis

A hierarchical agglomerative cluster analysis was used to identify patterns in the distribution of different oxides in Shadow Vlei. The dendrogram in Figure 12 shows the clusters into which each sample was classified and that the clusters were split at a height of 9 as the resultant clusters represented the sample heterogeneity in an effective way. There were a total of 5 clusters that contained between 25 and 3 samples. Clusters 1 and 2 contained about 67.5 % of the samples while Clusters 3, 4 and 5 contained approximately 19.5 %, 9.00 % and 4.00 % respectively.

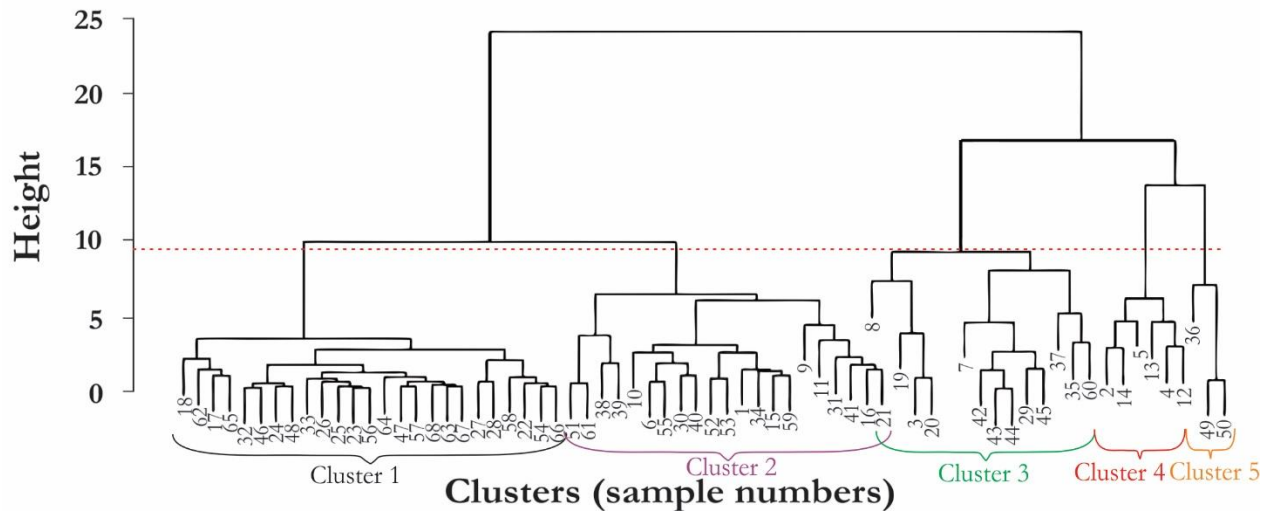

Figure 12: Dendrogram showing the grouping of individual samples into five clusters based on sample chemistry. Cluster colours are consistent with those in Figure 13, 14 and 15 (biplot). N=68.

The clusters were split predominantly based on variation in Al_2O_3, Fe_2O_3 and SiO_2 weight percentage values as they are the most predominant elements in the system and account for most of the variation in the geochemistry of Shadow Vlei. Cluster 1 contains samples that are rich in SiO_2 and have very low Al_2O_3 and Fe_2O_3 concentrations. The mean weight percentage for this cluster is 94.1 % for SiO_2, 1.60 % for Fe_2O_3 and 2.26 % for Al_2O_3 (Table 1). The weight percentage

means of SiO_2, Al_2O_3 and Fe_2O_3 in cluster 1 are significantly different to the means in all the other clusters (Table 2). Cluster 2 contains samples that have slightly lower SiO_2 concentrations ($\overline{x}$ = 85.2 %) and slightly higher Al_2O_3 ($\overline{x}$ = 4.84 %) and Fe_2O_3 ($\overline{x}$ = 4.16 %) concentrations. The mean weight percentages in cluster 2 are significantly different to all other clusters except in the case of Al_2O_3 where the mean in cluster 2 is not significantly different to its mean in cluster 5 (Table 2). The third cluster contains intermediate concentrations of SiO_2, Al_2O_3 and Fe_2O_3 ($\overline{x}$ = 73.5 %, 8.76 % and 6.80 % respectively) and is the cluster that is the most variable as this cluster holds the highest standard deviation values across all three oxides (Table 1). The means from cluster 3 are significantly different to those in all other clusters except in the case of Al_2O_3, where the difference between the means of cluster 3 and cluster 5 are not significant (Table 2). The highest mean weight percentage for Al_2O_3 is contained in cluster 4 ($\overline{x}$ = 12.9 %), which has mean values of 10.5 % and 61.5 % for Fe_2O_3 and SiO_2 respectively. The means in cluster 4 are significantly different to all other clusters except in the case of SiO_2 where the means in clusters 4 and 5 do not differ significantly. The highest mean weight percentage for Fe_2O_3 is contained within cluster 5 ($\overline{x}$ = 21.8 %) while the lowest mean concentration of SiO_2 is also contained in this cluster ($\overline{x}$ = 61.2 %).

Table 1: The mean weight percentages, standard deviations and sample number (Total N = 68) for Al_2O_3, Fe_2O_3 and SiO_2 across the five clusters. Values in **bold** are the maximum values for each column.

	Al_2O_3		**Fe_2O_3**		**SiO_2**		
Cluster	**Mean ($\overline{x}$)**	**Std. Dev.**	**Mean ($\overline{x}$)**	**Std. Dev.**	**Mean ($\overline{x}$)**	**Std. Dev.**	**N**
Cluster 1	2.26	0.76	1.60	0.60	**94.1**	1.64	25
Cluster 2	4.84	1.70	4.16	2.17	85.2	2.56	21
Cluster 3	8.76	**2.47**	6.80	**2.95**	73.5	**3.64**	13
Cluster 4	**12.9**	1.15	10.5	1.20	61.5	3.57	6
Cluster 5	7.02	1.72	**21.8**	0.69	61.2	2.79	3

All eleven oxides were included in the principal components analysis (PCA) such that there were eleven principal components (seven of which are displayed in Table 3). Principal component 1 accounts for 49.3 % of the variation in the samples and is strongly determined by the concentration of SiO_2 and Al_2O_3 in the sample (Figure 13). This means that samples that have high component 1 scores will have high SiO_2 concentrations and these concentrations will decrease as component 1 scores decrease. Conversely, Al_2O_3 concentration is highest for samples with low component 1 scores, and concentration decreases as component 1 scores increase. Principal component 2 on the other hand, accounts for 21.2 % of the variation in the samples and this component is determined almost entirely by the concentration of Fe_2O_3 in each sample. Samples that have low

component 2 scores have high Fe_2O_3 concentrations whereas those with high component 2 scores have low Fe_2O_3 concentrations. Principal components 1 and 2 account for the largest variation in the chemical composition of samples, with a cumulative 70.5 % of the variation in soil chemistry accounted for. Principal components three and four only account for 8.87 % and 6.66 % of the variation in the dataset respectively, and for the purposes of this study this was not considered sufficient to justify further investigation.

Table 2: Post-hoc comparisons using Tukey's HSD test. Differences between weight percentage means are shown where * indicates difference is significant at the 0.05 level, ** indicates difference is significant at the 0.01 level, *** indicates difference is significant at the 0.001 level.

			Al_2O_3		
	Cluster 1	**Cluster 2**	**Cluster 3**	**Cluster 4**	**Cluster 5**
Cluster 1	0	2.58***	6.50***	10.6***	4.76***
Cluster 2		0	3.92***	8.07***	2.18
Cluster 3			0	4.15***	1.74
Cluster 4				0	5.89***
Cluster 5					0
			Fe_2O_3		
	Cluster 1	**Cluster 2**	**Cluster 3**	**Cluster 4**	**Cluster 5**
Cluster 1	0	2.57*	5.20***	8.88***	20.3***
Cluster 2		0	2.64*	6.32***	17.7***
Cluster 3			0	3.68**	15.0***
Cluster 4				0	11.3***
Cluster 5					0
			SiO_2		
	Cluster 1	**Cluster 2**	**Cluster 3**	**Cluster 4**	**Cluster 5**
Cluster 1	0	8.89***	20.6***	32.7***	33.0***
Cluster 2		0	11.7***	23.9***	24.1***
Cluster 3			0	12.1***	12.4***
Cluster 4				0	0.29
Cluster 5					0

From Figure 13 it can be seen that clusters 1 to 4 are arranged systematically with decreasing component 1 scores. This distribution along component 1 is clearly associated with decreasing average SiO_2 concentrations and increasing average Al_2O_3 concentrations, as clearly reflected in Table 1. Although there seems a systematic increase in Fe_2O_3 concentration from clusters 1 to 5 (Table 1), clusters 2 and 3 are variable in their Fe_2O_3 concentration as indicated by the high standard deviations relative to the mean and their widespread distribution in relation to component 2. Looking at Figures 14 and 15, clusters 2 and 3 are spread laterally across the cross-sections and are 'transitional' samples as they often separate samples in cluster 1 from samples in clusters 4 and 5. The positioning of the samples in cluster 4 in Figure 13, with low component 1 scores is largely

accounted for by high concentrations of Al_2O_3 and low concentrations of SiO_2, while the three members of cluster 5 have low component 2 scores as a result of very high concentrations of Fe_2O_3.

Table 3: Results from the covariant PCA showing standard deviation, proportion of variance and the cumulative proportion of variance in seven of the eleven principal components.

	Comp. 1	Comp. 2	Comp. 3	Comp. 4	Comp. 5	Comp. 6	Comp. 7
Std. Dev	2.33	1.53	0.988	0.856	0.736	0.666	0.628
Proportion of Variance	0.493	0.212	0.0887	0.0666	0.0493	0.0403	0.0359
Cumulative Proportion	0.493	0.705	0.794	0.860	0.910	0.950	0.986

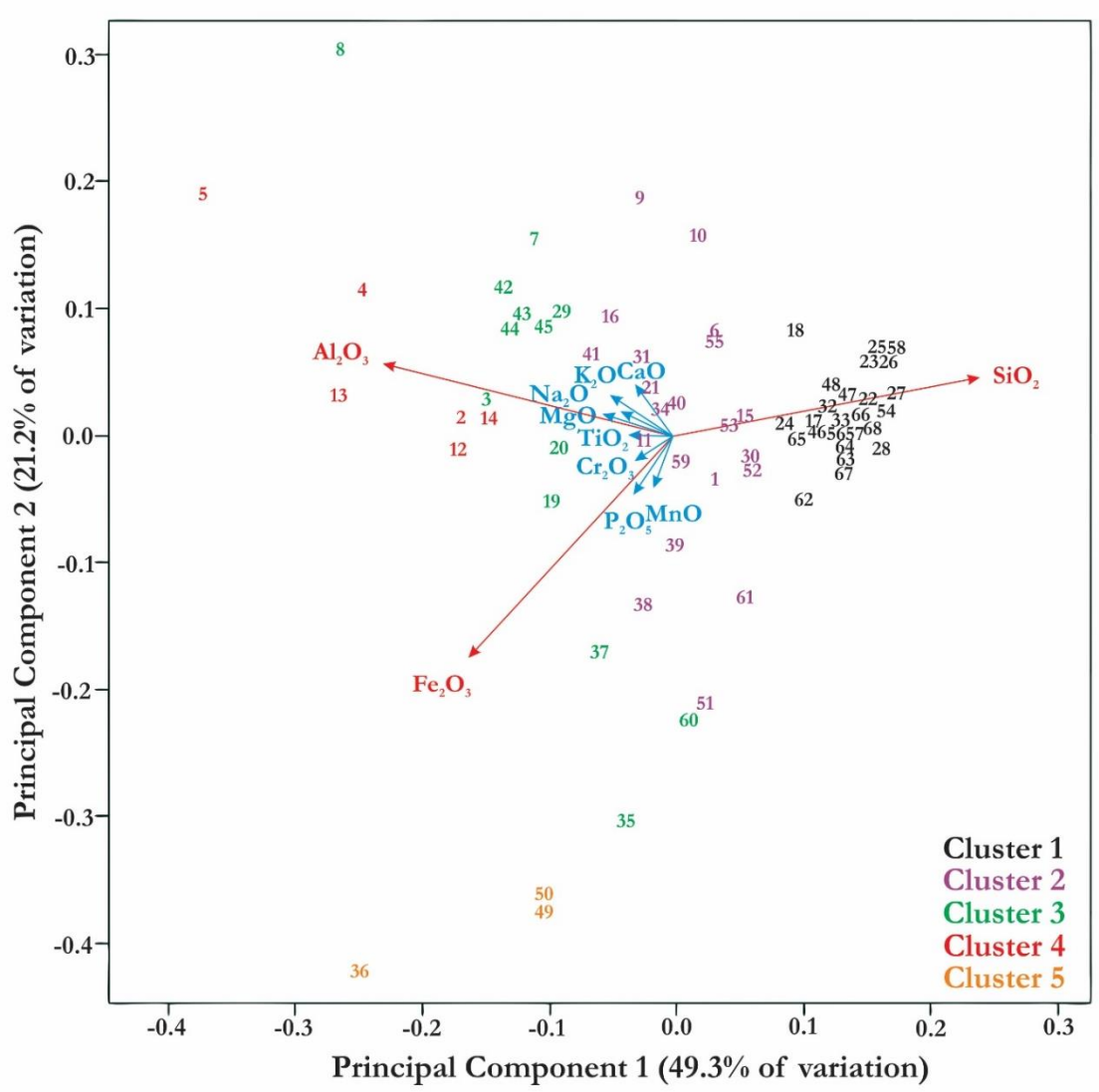

Figure 13: Biplot from the principal components analysis (PCA). Distance between sample numbers is coarsely related to their chemical similarity, the length of the arrows approximates the standard deviation of the underlying chemical variables. Numbers are coloured with cluster codes from the cluster analysis. N = 68.

6.2.1.3 Variation in soil chemistry in relation to depression morphology

There is a clear link between the morphology of Shadow Vlei and the distribution of SiO_2, Al_2O_3 and Fe_2O_3 (Figures 14 and 15). Al_2O_3 and Fe_2O_3 are concentrated beneath the mounds that form the margins of the depression whereas SiO_2 is found in significantly lower concentrations in these regions. Fe_2O_3 is concentrated close to the surface in the margins of the depression with concentrations often reaching above 12 %. It is moderately concentrated near the soil surface beneath the centre of the depression with concentrations that range between 4 % and 8 %. Fe_2O_3 is depleted with increasing depth and increasing distance away from the margins of the depression with average concentrations that are less than 1 % (see Figures 14B and 15B).

Al_2O_3 has a similar distribution to Fe_2O_3 but is present at more uniform concentrations beneath the centre of Shadow Vlei. Al_2O_3 is also concentrated beneath the margins of the wetland, also reaching concentrations greater than 12 %. However, Al_2O_3 exists in higher concentrations at depth than Fe_2O_3 does (see Figures 14A and 15A). The concentration of the of SiO_2 is distributed inversely to Al_2O_3 and Fe_2O_3, where SiO_2 is present at the lowest concentrations beneath the margins of the depression, where it occurs at concentrations that range from 55 % to 70 %. However, in the surrounding landscape and with increasing depth, SiO_2 generally occurs at concentrations that are greater than 85 %.

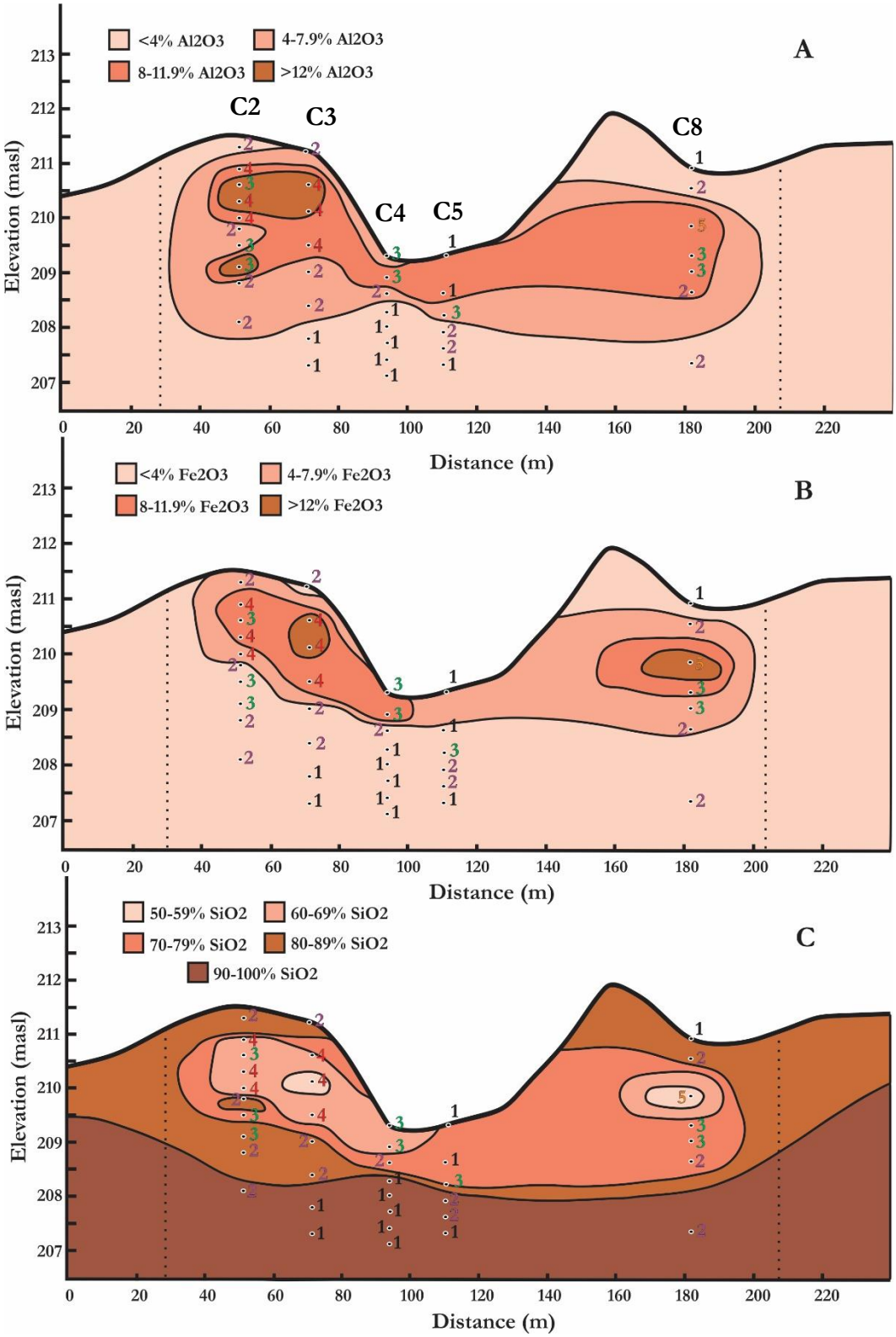

Figure 14: Cross-section showing distribution of Al_2O_3 (**A**), Fe_2O_3 (**B**) and SiO_2 (**C**) beneath Shadow Vlei (data taken from first transect line). Dots represent the vertical and horizontal positions of individual samples taken from the cores and the coloured numbers represent the cluster number that each sample was assigned using a hierarchical agglomerative cluster analysis. Dashed lines represent areas where there is interpolated data. Core numbers are depicted in **A**.

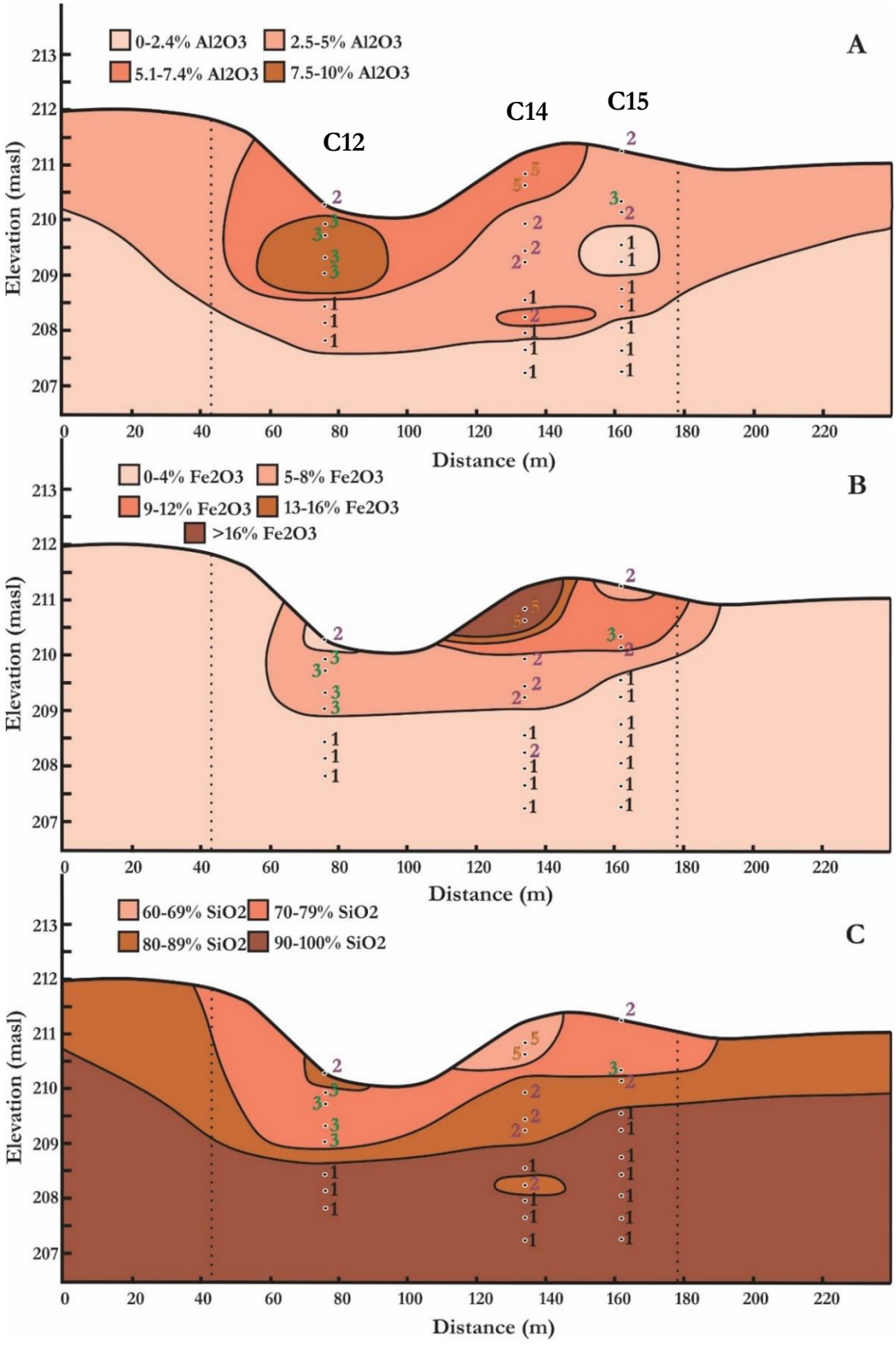

Figure 15: Cross-sections showing distribution of Al_2O_3 (**A**), Fe_2O_3 (**B**) and SiO_2 (**C**) beneath Shadow Vlei (data taken from second transect line). Dots represent the vertical and horizontal positions of individual samples taken from the cores and the coloured numbers represent the cluster number identified in the hierarchical agglomerative cluster analysis. Dashed lines represent areas where there is interpolated data. Core numbers are depicted in **A**.

6.2.1.4 Variation of, and relation between SiO_2, Al_2O_3 and Fe_2O_3

The relationship between SiO_2 and Fe_2O_3 is depicted in Figure 16A, which shows an inverse relationship (R^2 = 0.6497). A similar inverse relationship exists between Al_2O_3 and SiO_2, as low concentrations of SiO_2 are most often associated with high concentrations of Al_2O_3 (R^2 = 0.8003; Figure 16B). It is probable that the predictable nature of this relationship is a result of the fact that both silicon and aluminium are very stable elements and their movement below ground is relatively predictable. The direct relationship that exists between Al_2O_3 and Fe_2O_3 is much less predictable (R^2 = 0.2962; Figure 16C) and this is probably a result of the unpredictable nature of Fe_2O_3 as it is easily affected by redox conditions and can be mobilized and redistributed in a relatively random manner.

6.3 Variation in mineralogy of Shadow Vlei

The mineralogy of Shadow Vlei is relatively simple as the system has undergone a long process of weathering. Quartz (SiO_2) is the most abundant mineral in the depression ($\overline{x}$ = 84.0 %, Table 4) as it is extremely resistant to weathering. The concentration of quartz in the mineralogy is clearly related to the concentration of SiO_2 (Figure 17A) but only 62.37 % of the variation in the concentrations of SiO_2 is explained by quartz. Some of the residual variation in SiO_2 may be explained by the presence of other silicon containing minerals such as feldspars, muscovite and clay minerals.

Table 4: Mineralogy of 23 selected samples (displayed as weight % of entire sample). The n value in column four denotes the frequency which that phase occurred in the 23 samples.

Mineral	Mean (wt%)	Standard Deviation	Count (n)
Quartz	84.0	10.4	23
Muscovite	4.1	2.3	23
Orthoclase	5.1	3.0	18
Calcite	3.2	2.3	5
Montmorillonite	2.2	1.5	16
Magnesite	2.0	1.1	4
Albite	2.5	0.5	2
Kaolinite	3.7	2.5	17
Goethite	7.8	4.3	12
Anorthite	3.8	2.1	4

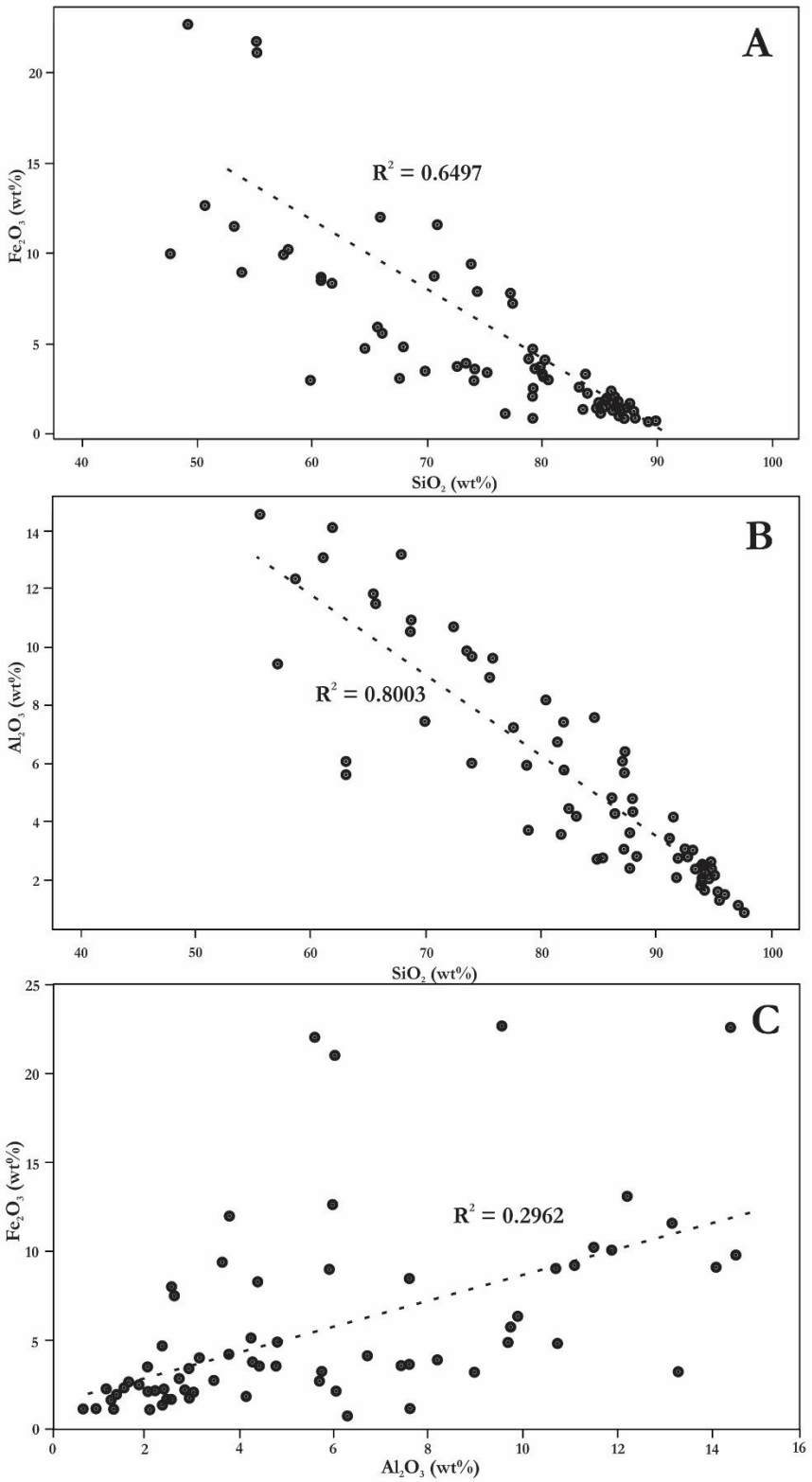

Figure 16: (A) SiO_2 weight percentage vs. Fe_2O_3 weight percentage, (B) SiO_2 weight percentage vs. Al_2O_3 weight percentage, (C) Al_2O_3 weight percentage vs. Fe_2O_3 weight percentage. Data taken from XRF results, N = 68.

Muscovite ($KAl_3Si_3O_{10}(OH)_2$) is a common mineral in Shadow Vlei ($\overline{x}$ = 4.1 %), occurring in all the samples analysed, while the mineral orthoclase ($KAlSi_3O_8$) with a mean weight percentage of 5.1 % occurred in 18 of the samples. A third aluminium containing mineral, kaolinite ($Al_2Si_2O_5(OH)_4$), with an average abundance of 3.7 %, was also present in many samples. The abundance of muscovite, orthoclase and kaolinite is related to the concentration of $Al2O_3$ beneath the depression (Figure 17B). Kaolinite is a common product of weathering in sandstones and is a common end product of the weathering of both muscovite and feldspars. Montmorillonite ($(Ca,Na,H)(Al,Mg,Fe,Zn)_2Si_4O_{10}(OH)_2 \cdot 8H_2O$) is a common smectite clay mineral in Shadow Vlei, although it only ever occurs in very small concentrations ($\overline{x}$ = 2.2 %). Goethite (FeO(OH)), with an average concentration of 7.8 %, was found in 12 of the samples. The presence of goethite, which is most abundant in the marginal areas of the depression, is correlated (R^2 = 0.7708) to the presence of $Fe2O_3$ in the chemistry (Figure 17C).

The two parent material samples that were extracted were predominantly composed of quartz ($\overline{x}$ = 92 %) and orthoclase ($\overline{x}$ = 4 %) with negligible concentrations of kaolinite and muscovite. No XRF was conducted on the parent material samples but deriving an approximate chemistry from the mineralogy is simple. Therefore, parent material from which the current geochemistry of Shadow Vlei is derived can be likened to the composition of samples in cluster 2 in terms of their SiO2 and $Al2O_3$ content (Table 1). The parent material is very rich in silica which predominantly occurs as quartz but will also occur in the other aluminosilicate minerals. The $Al2O_3$ exists in mineral form as either feldspars, clay minerals or muscovite whereas the $Fe2O_3$ in the parent material would exist as a thin layer of Fe^{3+} that coats each individual sand grain in the sandstone lattice – giving it it's commonly characteristic brick red colour. It is unlikely that $Fe2O_3$ occurs at concentrations greater than 2 % or that aluminium exists at concentrations greater than 5 % in the parent material. Therefore, it is quite remarkable how heterogenous the geochemistry of Shadow Vlei is in relation to the simplicity of the bedrock from which it is derived. The origin and evolution of Shadow Vlei has been fundamentally controlled and moulded both by geomorphic and geochemical processes and it can only be truly understood using geomorphic and geochemical explanations.

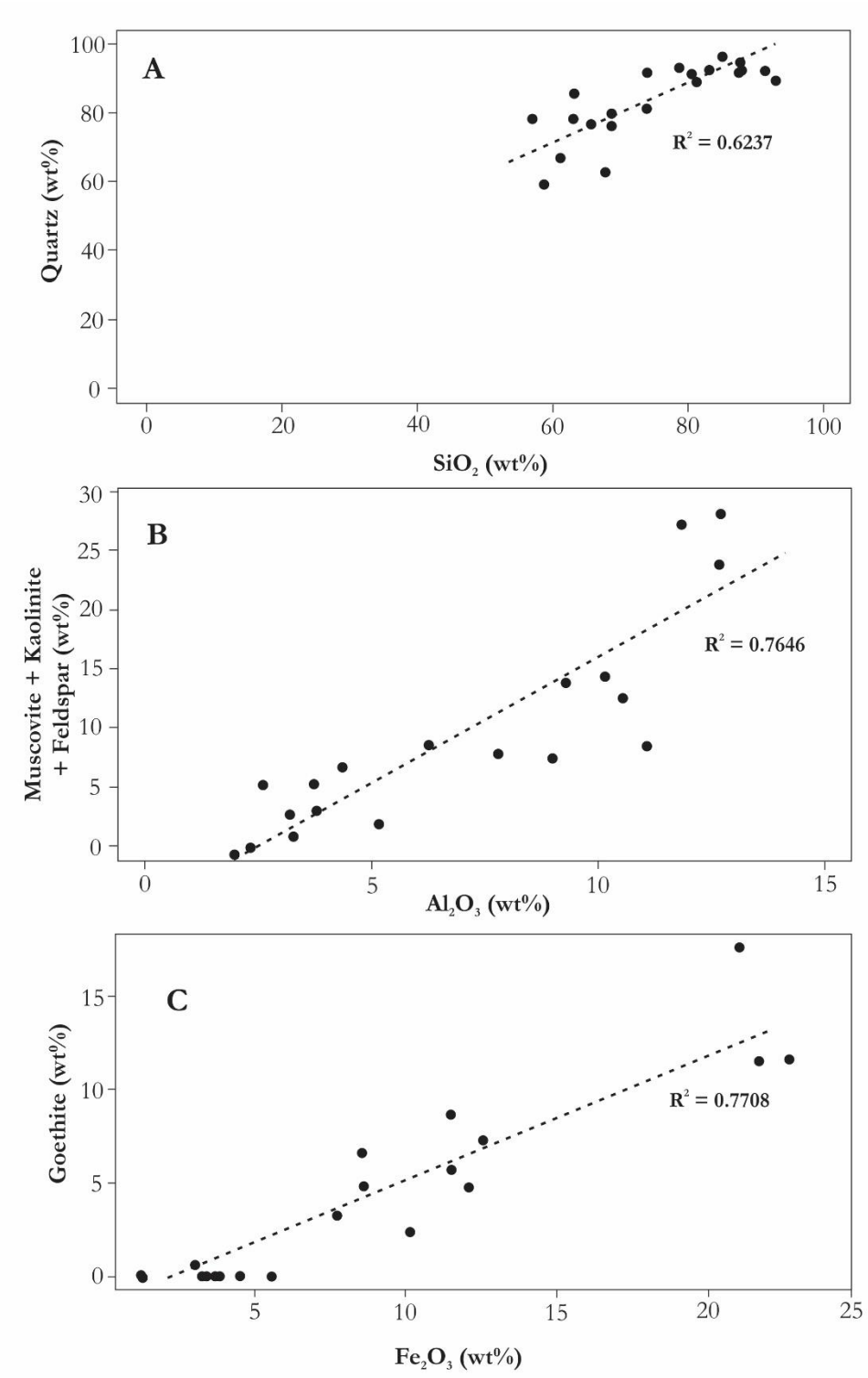

Figure 17: Correlation between mineralogical and chemical analyses. (A) SiO_2 vs. Quartz, (B) Al_2O_3 vs. sum of Muscovite, Kaolinite and Feldspars, (C) Fe_2O_3 vs. Goethite.

7 Discussion

7.1 Conceptualising the likely origin of Shadow Vlei

The scientific examination of the geomorphic origin of wetlands is still in its infancy and there are still many mechanisms of wetland formation that are poorly understood (Tooth and McCarthy, 2007). Therefore, much of the work on the geomorphic origin and evolution of wetlands can only be considered based on a limited amount of published research material, meaning that much of this work is exploratory and producing concepts that have not been considered before. One of the key reasons why geomorphic research in wetlands is so important is that it allows wetland scientists to consider the origin, evolution and potential future trajectories of change in wetlands over extended periods: it becomes possible to understand a wetland in terms of broader landscape processes that may have a bearing on "what might happen next?". The importance of considering the role of time in wetland structure and function is often considered irrelevant by wetland scientists, but evidence from this study points to the fact that Shadow Vlei has formed over a long period of time and that its structural evolution is closely tied to processes that are confined to below ground.

The model of formation of depression wetlands proposed by Goudie and Thomas (1985) has laid the foundation for our current understanding of the formation of these systems. Their theory of endorheic depression formation still seems valid in many contexts in arid and semi-arid environments, and it was only with an understanding of Goudie and Thomas's wetland formation model that Edwards *et al.* (2016) and Alistoun (2014) could question and critically engage with the origin of the wetlands that they studied. An engagement with all three wetland origin models has led to the formulation and testing of the model that will be presented here.

The wetland formation model that was presented by Goudie and Thomas (1985) cannot be applied to Shadow Vlei for several reasons. The first is that Shadow Vlei is distinctly atoll shaped, suggesting that there has been both aggradation and degradation (sagging). In a wetland where sediment is being removed solely by aeolian processes, the creation of a large topographic feature downwind of the depression might be observed, but it is unlikely that positive relief would be created evenly around the entire wetland in the way that it has been in Shadow Vlei. The resistant nature of the sandstone lithology upon which Shadow Vlei is located means that removal of sediment by wind or biotic processes is also unlikely. Erosion by wind might account for a small amount of sediment removal – especially fine sand, fine-grained silts or clays – but it is unlikely to

explain the relief that has been created all the way around Shadow Vlei. A further reason for questioning the validity of the Goudie and Thomas (1985) model in explaining the origin of Shadow Vlei is that it is in an area that normally receives sufficient rainfall to support permanent ground covering vegetation, particularly as the area receives rainfall in every month of the year (Mucina and Rutherford, 2006). Although the rainfall received in the area is not significantly greater than what defines a semi-arid climate, there is enough moisture in the area to sustain sufficient vegetation to prevent erosion by wind. Removal of sediment by animals has possibly contributed to the downward sagging of the centre of the depression but cannot explain the uniformly raised margins of the wetland. The presence of ferricrete all the way around the depression margin also suggests that biogeochemical rather than aeolian processes are likely to have contributed to the formation of the depression wetland feature with an elevated margin. It is for these reasons that an alternative model of wetland formation needs to be suggested for many of the depression wetlands that exist on the African Erosion Surface of the southern Cape Coast.

7.2 Chemical background: iron cycling (ferrolysis)

The process of sagging and volume loss that is observed in the centre of Shadow Vlei, and the swelling in the depression margin, is likely to be a consequence of processes related to iron chemistry, particularly in environments with oxidizing and reducing conditions in close proximity to each other, or where there are alternating oxidizing and reducing conditions. Given that flooded soils are anaerobic and therefore dominated by reduction reactions, and that non-flooded soils are oxidizing (Mitsch and Gosselink 2015), such conditions are likely to exist in and adjacent to Shadow Vlei in response to alternating high and low water levels.

The process of ferrolysis was first conceptualised by Brinkman in 1970 as a soil forming cycle that is responsible for clay destruction, strong texture contrasts in duplex soils and interlayering of clay minerals, all as a result of iron redistribution below ground. Iron commonly exists in all soils and is a common constituent of sedimentary rocks with concentrations that range between <0.1 % and >50 % (Schwertmann, 1991). Iron can exist in surface soils as mottles, concretions, bands and as coatings of individual sand grains in sandstones. It commonly occurs as Fe^{3+} (ferric iron or iron(III)) and less commonly as Fe^{2+} (ferrous iron or iron(II); Schwertmann, 1991). Ferrolysis describes a cyclical process whereby iron is constantly being changed from its ferric state to its ferrous state and back again. The transformation of ferric iron to ferrous iron is a reduction reaction that occurs when Fe^{3+} accepts an electron from an electron donor and is changed to Fe^{2+}. Ferrous iron is transformed to ferric iron during an oxidation reaction where Fe^{2+} donates an

electron to oxygen (Equation 4). The reduction of ferric iron generally occurs in waterlogged, anaerobic soils where Fe^{3+} can become a primary electron acceptor, and the oxidation of ferrous iron occurs in well drained, aerobic soils where Fe^{2+} is exposed to oxygen and can act as a primary electron donor.

The process of ferrolysis is therefore dependent on a seasonally fluctuating water table. During the oxidizing phase of ferrolysis, Fe^{2+} is oxidised to Fe^{3+} as it reacts with molecular oxygen and residual moisture in the soil to form a ferric oxyhydroxide such as goethite (FeO(OH)) or hydrated iron oxide ($Fe(OH)_3$) (Van Ranst and De Coninck, 2002). The reaction that occurs during oxidation of Fe^{2+} produces acidity in the form of H^+ ions and is responsible for lowering the pH in the soil profile during dry periods when oxygen diffuses into the soil profile (Equation 4; Mann, 1983). The H^+ ions and resultant reduction in pH that are produced during this reaction are thought to be responsible for the disintegration of clay minerals. Acid corrodes the tetrahedral and octahedral layers of clay lattice structures and is responsible for the removal and leaching of exchangeable cations such as Ca^{2+}, Na^+, Mg^{2+}, K^+, Al^{3+} and even Si^{4+} in some cases (Brinkman, 1979).

Equation 4: Simplified oxidation of ferrous iron to produce goethite and acidity

$$4Fe^{2+} + 6H_2O + O_2 \rightarrow 4FeO(OH) + 8H^+$$

The reducing phase of ferrolysis is initiated when the soil or rock profile becomes saturated with water after a rainfall event and anaerobic conditions are created. Anaerobic conditions occur during waterlogged phases because the diffusion of oxygen in aqueous solutions can be up to 10000 times slower than in porous and well drained-soils (Mitsch and Gosselink, 2015). Soil microbes and bacteria present in the soil profile require a steady source of oxygen to survive and will quickly consume the oxygen trapped in the soil profile after saturation. Once the atmospheric oxygen is consumed, microbes will turn to other oxygen containing compounds and minerals as sources of oxygen. The consumption of carbohydrates in organic substrates by microbes (Equation 5) produces electrons which are then used by microbes to reduce other oxygen containing compounds such as nitrates (NO_3), manganese bearing compounds (MnO_2), iron containing compounds ($Fe(OH)_3$, FeO(OH)) and sulfates (SO_4).

Equation 5: A reaction that describes microbial oxidation of carbohydrates in organic substrates as electron donors. $n \geq 1$.

$$[CH_2O]n + nH_2O \rightarrow nCO_2 + 4ne^- + 4nH^+$$

During anaerobic phases, soil microbes will preferentially reduce certain compounds based on their redox potentials. Reddy and D'Angelo (1997) describe this process where atmospheric

oxygen present in the soil is quickly consumed subsequent to soil waterlogging as microbes oxidise organic substrates. After oxygen depletion, soil microbes will reduce nitrates, which become electron acceptors at a redox potential of approximately +250 mV. As the redox potential decreases, manganic compounds are reduced to manganous compounds as they become sensitive to reducing conditions at about +225 mV (Reddy and D'Angelo, 1997). Ferric iron is then reduced to ferrous iron when the redox potential in the soil ranges between +100 mV and -100 mV (Equation 6). After the reduction of iron, sulphides are produced from the reduction of sulphates as they become sensitive to redox potentials between -100 mV and -200 mV.

Equation 6: Simplified reduction reaction of ferric iron to produce ferrous iron in waterlogged soils

$$FeO(OH) + e^- + 3H^+ \rightarrow Fe^{2+} + 2H_2O$$

The cycle of ferrolysis is complete when the soil becomes aerobic once the water table drops again during the dry season. This leads to the oxidation of soluble ferrous iron to produce insoluble ferric oxyhydroxides, at which time acidity increases once again.

7.3 Iron cycling in the context of the origin and development of Shadow Vlei

During its early formation, the depth of Shadow Vlei might have been measured in decimeters, and the diameter in meters to tens of meters. Provided that inundation of such a shallow and small depression was for sufficiently long to promote the presence of anaerobic conditions in the soil, dissolution of iron would have been initiated in the near-surface weathering soil environment during flooding. At this point, and provided localised recharge of groundwater is taking place from the depression, iron moves away from the centre of the depression where the soil that is permanently to semi-permanently flooded. As such, the near-surface soils at the centre of the shallow depression would become depleted in iron. However, as a result of increased oxygen availability in the soil when the water table drops, ferrous iron would precipitate from solution in the near-surface soil environment in the centre of the depression, and because of lateral movement of dissolved ferrous iron from the more permanently flooded soils beneath the centre of the depression, iron would precipitate from solution to form a shallow localised feature at the edge of the depression. It is very possible that this iron-cycling process has been, and still is, responsible for the enlargement of Shadow Vlei as iron is continually being moved from the centre towards the margins of the depression, where it is deposited. Over long periods of time, through many cycles of oxidation and reduction, the margins of the depression have become iron rich as the centre has become increasingly iron poor, and this trapping of iron in the margins of the depression

has led to ferricrete formation and aggradation of the margins. The process of ferrolysis can explain the concentration of iron in the form of goethite as well as the depletion of clay minerals in the marginal area of Shadow Vlei.

Ferrolysis occurs primarily in the marginal areas of the wetland for several reasons. The process requires a constant supply of iron, and the movement of iron from the centre towards the margins of the depression due to groundwater recharge provides an ideal source. There are still small amounts of iron in the centre of the depression, which means that there is still potential for the transferral of more iron into the margins. Such movement would cause further sagging in the centre and aggradation in the margins simultaneously.

Ferrolysis will only occur where there is microbial activity, and microbial activity will only be constant in an area where an organic substrate is produced in relative abundance. The central and marginal areas of Shadow Vlei are always vegetated, therefore there will be a sufficient supply of decomposable material for soil microbes to use as electron sources. Ferrolysis requires a fluctuating water table that exists below-ground, where both aerobic and anaerobic conditions can be created. The local water table in the marginal areas of Shadow Vlei is deep enough below ground for both aerobic and anaerobic conditions to occur, is close enough to an organic substrate production zone and has a constant and steady supply of iron. The combination of chemical weathering in the centre, and ferrolysis and ferricrete formation in the margins of Shadow Vlei, has led to a combined sagging/aggradation effect that has created sufficient relief to form a depression wetland.

7.4 Evidence of ferrolysis in Shadow Vlei

The multi-step process of ferrolysis is comprised of many variables that act together to create conditions that redistribute iron in a soil profile. These many steps are characterised by changes in soil geochemistry, mineralogy, soil colour, soil texture pH and Eh and the measurement and observation of these changes in the soil profile can act as evidence for ferrolysis in Shadow Vlei.

7.4.1 The presence of extensive ferricrete outcrops in the margins of Shadow Vlei

The process of iron-cycling as described in ferrolysis can explain the widespread occurrence of ferricrete in the marginal areas of Shadow Vlei as the occurrence of ferricrete is commonly associated with a fluctuating water table as it is reliant on the redistribution and accumulation of iron (Pain and Ollier, 1992; Phillips *et al.*, 1997). Ferricrete duricrusts are often located a short vertical distance above the average elevation of the water table as iron is extremely sensitive to

oxidising conditions and will precipitate out of solution almost immediately upon exposure to oxygen. The occurrence of ferricrete in the marginal areas of depression wetlands has been widely documented in both Australia and the United States and is said to be a direct result of lateral transport of iron in ground water and exposure of iron to oxidising conditions (Pain and Ollier, 1992). These ferricrete duricrusts associated with depressions are rarely thicker than 2 m but can cover large horizontal areas depending on the extent of the iron supply. The ferricrete in Shadow Vlei is widespread on the eastern margin of the wetland and is not thicker than 2 m at any point. Goethite is a common cementing agent in ferricrete and the widespread presence of goethite in the margins of Shadow Vlei is indicative of ferricrete formation (Phillips, 2000). The occurrence of goethite near or on the land surface is associated with acidic ground water conditions, alternating redox conditions and a fluctuating water table – all of which can be attributed to the ferrolysis process (McQueen, 2005). However, ferrolysis and ferricrete formation have never been explicitly linked in the literature, but several studies have acknowledged the role of ferrolysis in creating conditions conducive for laterite and ferricrete formation (Mann, 1983; Ambrosi *et al.*, 1986; Lee and Gilkes, 2005). During the early stages of development, Shadow Vlei would have been characterised by small ferricrete outcrops in the marginal areas and as the process of iron-cycling progressed, the ferricrete outcrops would have moved farther away from the depression centre due to iron recycling from the inner zone of the ferricrete deposits towards the outer edge of the deposits. As this recycling took place, more iron would have been captured due to deepening and broadening of the weathering front.

The creation of positive relief has been attributed to the formation of ferricrete in Australia (Conacher *et al.*, 1991; Pain and Ollier, 1992), in Mali and Burkina Faso (Butt and Bristow, 2013) and in Central Sudan (Schwarz, 1994) in seasonally wet conditions. Ferricrete creates positive relief both as a consequence of the accumulation and consolidation of ferruginous material in a single location (in this case in the depression margin), leading to swelling, and also as a consequence of the lowering of the surface due to volume losses associated with weathering. Because ferricrete is composed primarily of very resistant iron rich cement such as goethite, hematite or limonite, it is not easily eroded or weathered in aerobic conditions and is therefore associated with 'relief inversion' where less resistant material surrounding the ferricrete weathers and erodes to create positive relief where ferricrete exists.

7.4.2 Clay destruction and iron-aluminium substitution in goethite

The creation of acidity during the oxidation of Fe^{2+} (Equation 4) can be responsible for the liberation of exchangeable cations such as Ca^{2+}, Na^{+}, Mg^{2+}, K^{+}, Al^{3+} and Si^{4+} from clay lattice structures, and hence the disintegration of clay minerals (Brinkman, 1979). 2:1 clays such as montmorillonite disintegrate faster than 1:1 clays, such as kaolinite, because 2:1 clays generally have a higher cation exchange capacity (CEC) than 1:1 clays. This means that the clay lattice structures of 2:1 clays have more potential binding sites for H^{+} ions, whereby displacement of an exchangeable cation from the clay structure will occur (Brinkman, 1970). The removal of Al^{3+} from clay minerals can commonly occur during the oxidation phase of ferrolysis and can be substituted out of the clay structure by either H^{+} or Fe^{3+} ions. These aluminium ions can either be leached out of the soil profile at the beginning of the reducing phase or they will precipitate from solution at this point to form aluminium oxyhydroxides with the release of hydroxide ions from iron rich minerals (Van Ranst and De Coninck, 2002). Silicon can also be removed from a clay structure when the tetrahedral layers of clays are exposed through repeated removal of other exchangeable cations. Silicon can be dissolved in acidic conditions created by ferrolysis and can be transported in solution to precipitate as amorphous silica elsewhere in the soil profile (Brinkman, 1970). This process of silicon redistribution in the ferrolysed soil profile could partly account for the very low SiO_2 concentrations in the marginal areas of Shadow Vlei (Figures 14 and 15). The low concentrations of SiO_2 in the ferrolysed zone could be explained both by the removal of SiO_2 from this zone as well as the dilution of SiO_2 as a result of the net inundation of the soil by iron and aluminium ions in the marginal areas of the depression. The samples with the lowest clay fractions were all located in the margins of Shadow Vlei where the highest concentrations of goethite were observed, and this is indicative of acidic conditions that are created during ferrolysis.

It is common for Al^{3+} to substitute for Fe^{3+} to form aluminium rich goethite or hematite and many studies have confirmed that in moderate to strongly acidic soils, aluminium rich goethite can account for up to 23% of all goethite found in the soil profile (Fitzpatrick and Schwertmann, 1982). Al^{3+} has a smaller atomic radius than Fe^{3+} and therefore can easily substitute the iron in goethite or hematite, which is common in acidic conditions because Al^{3+} will be made readily available through the disintegration of clay minerals (Fitzpatrick and Schwertmann, 1982). The substitution of aluminium into goethite minerals could explain the complex relationship between aluminium and iron concentrations in the soil profile depicted in Figure 16C, as this process of substitution is difficult to predict.

7.4.3 The widespread existence of iron reducing bacteria

The reduction of ferric oxyhydroxides is only made possible by microbes and bacteria that reduce iron minerals in anaerobic conditions. The identification of specific iron reducing bacteria is not the focus of this study, but many other studies have shown that in the absence of sufficient electron acceptors, microbes will turn to reducing ferric iron in the soil profile to produce Fe^{2+} under anaerobic conditions (Johnson and McGinness, 1991; Luther *et al.*, 1992; Bridge and Johnson, 1998; Weber *et al.*, 2006). Bridge and Johnson (1998) tested the differing iron reducing capabilities of five moderately thermophilic and acidophilic bacteria in anaerobic conditions in a series of laboratory tests. The bacteria were grown in anaerobic cultures containing 20 mM ferric sulfate, 10 mM glycerol and 0.02 % yeast extract at a pH of 2.0. The growth dishes were incubated at 45 ^{o}C to decrease the reaction energy required for reduction of Fe^{3+}. The concentration of ferrous iron was less than 1 mM at the beginning of each experiment and was monitored throughout the experiment using colorimetry by the ferrozine assay. Each bacterium showed the ability to reduce ferric iron, though three species (*Sulfobacillus acidophilus* YTF1, *Sulfobacillus acidophilus* THWX and *Acidithiobacillus ferrooxidans* TH3) of bacteria were much more efficient than the other two (*Sulfobacillus acidophilus* ALV, *Sulfobacillus thermosulfidooxidans* TH1) (Figure 18). Although these experiments were conducted under laboratory conditions, the results show that there are species of bacteria that readily reduce ferric iron to produce ferrous iron under anaerobic conditions. During the reducing phase of ferrolysis, the soil pH can occasionally drop to a minimum of 3 but most commonly exists between 4 and 5 (Brinkman, 1979). The soil temperature will also infrequently reach temperatures above 30 ^{o}C and it should be noted that the results presented by Bridge and Johnson (1998) would overcompensate for the rate at which bacteria would reduce ferric iron under natural conditions. However, Weber *et al.* (2006) identified 45 different species of anaerobic iron reducing microorganisms that have all shown iron reducing capabilities in natural conditions. There is also evidence to show that microbes preferentially reduce poorly crystalline iron oxyhydroxides such as goethite as they are more sensitive to redox potentials than crystalline iron oxyhydroxides (Weber *et al.,* 2006). With a sufficient supply of organic substrate and anaerobic conditions, it is plausible that iron reduction by soil microbes is responsible for the dissolution of insoluble goethite in Shadow Vlei.

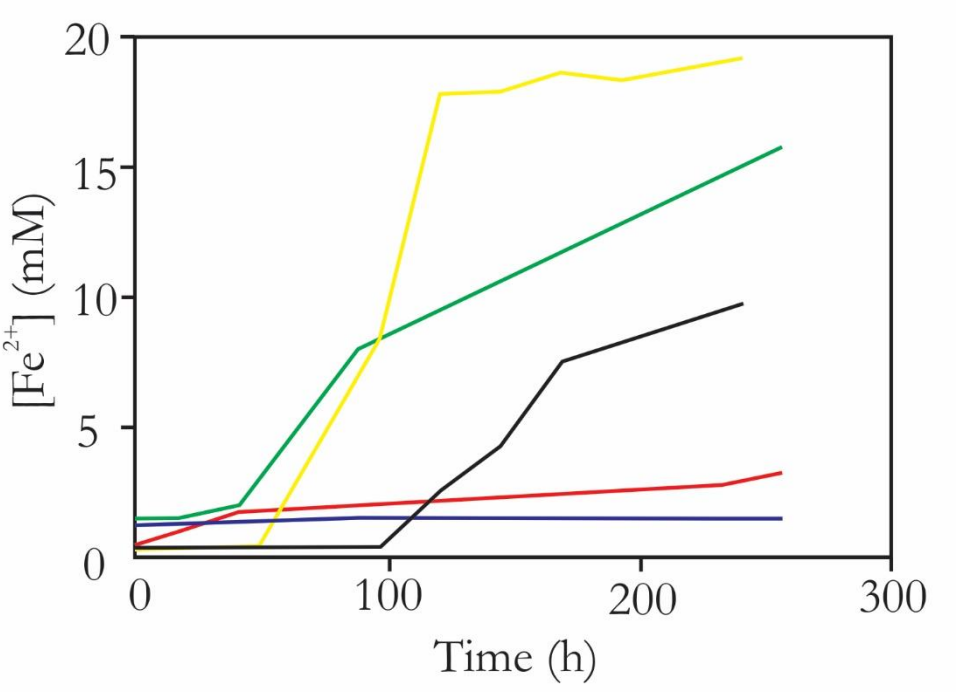

Figure 18: Reduction of ferric iron by strains of moderately thermophilic, acidophilic bacteria grown in anaerobic cultures. Symbols: , *Sulfobacillus acidophilus* ALV; , *Sulfobacillus acidophilus* THWX; , *Sulfobacillus acidophilus* YTF1; , *Sulfobacillus thermosulfidooxidans* TH1; , *Acidithiobacillus ferrooxidans* TH3 (adapted from Bridge and Johnson, 1998).

7.5 Later evolution of Shadow Vlei: The role of weathering and mineralogical simplification

The process of iron-cycling in reactions described by ferrolysis was responsible for the initiation of Shadow Vlei and the initial formation of positive relief in the wetland margins. However, as ferrolysis progressed, the repeated periodic inundation and desiccation of the depression created a zone where increased chemical weathering would have taken place. It is through the process of chemical weathering and mineralogical simplification that the clay minerals and the perched water table found in Shadow Vlei were formed, and volume loss occurred in the centre of the depression. Due to the lateral movement of water, dissolved solutes would have been transported from the centre of the depression towards the marginal areas. This lateral movement of dissolved solutes would have caused volume loss and sagging in the centre of the depression as material was slowly removed from this vicinity over long periods of time. The most soluble and exchangeable elements would have been removed first, including Ca^{2+}, Fe^{2+}, Na^{+}, Mg^{2+}, Mn^{2+} and K^{+} – such that simplification of the geochemistry and mineralogy occurred below the depression. In the case of Shadow Vlei, most of the soluble constituents of the geochemistry have been removed, and only very small proportions of these constituents remain in the soil and rock profiles beneath the centre or at great depths (>2 m) in the margins of the depression. Typically, it is the case that the more

soluble an element is, the longer it will stay in solution before it is precipitated out, such that the more soluble elements are moved much more efficiently than more insoluble elements (Taylor & Eggleton, 2001).

There are small proportions of the more soluble elements like K, Ca and Na in the geochemistry of Shadow Vlei – all of which are mineralogically present in feldspars such as orthoclase, albite and anorthite and in muscovite micas. Feldspars are common detrital constituents of sandstones and can comprise up to a maximum of 50 % of the total mineralogy in sandstone profiles, often being responsible for clay mineral formation in a weathered sandstone profile (Mcbride, 1963). The presence of muscovite in Shadow Vlei is somewhat anomalous as muscovite is much less commonly found in sandstones as a detrital constituent as muscovites would be chemically altered in the process of sandstone formation. However, feldspars can weather through the dissociation of K^+ ions to form an illite which is a fine-grained muscovite clay which acts as an intermediary mineral in the formation of kaolinite from feldspar (Equation 7 and 8; Dunlevey, *pers comm*). In a bulk powder XRD analysis, both illite and muscovite produce peaks at 10 Å, such that illite can easily be misinterpreted as muscovite. The proportion of muscovite to illite can be determined using centrifugal or settling disaggregation techniques as muscovite settles at a much slower rate than illite particles (Towe, 1974).

Equation 7: The dissociation of K^+ ions from orthoclase to form illite (~muscovite) and soluble silica.

$$3KAlSi_3O_8 + 2H^+ + 12H_2O \rightarrow KAl_3Si_3O_{10}(OH)_2 + 6H_4SiO_4 + 2K^+$$

Equation 8: Further dissociation of K^+ ions from illite to form kaolinite.

$$2KAl_3Si_3O_{10}(OH)_2 + 2H^+ + 3H_2O \rightarrow 3Al_2Si_2O_5(OH)_4 + 2K^+$$

This intermediary formation of illite could explain the concentrations of muscovite in the mineralogy of Shadow Vlei. Both feldspars and micas commonly weather to form kandite and smectite clay minerals like kaolinite or montmorillonite – both of which occur in Shadow Vlei (Millot, 2013). The highest concentrations of clay minerals are located in the centre of the depression where much of the weathering would take place. They are also indicative of a clay and bedrock perched water table described by Melly *et al.* (2017). There is a marked decrease in the concentrations of clay minerals in the margins of the depression and this could be explained by the process of ferrolysis as it is a process that can lead to the destruction of clay minerals in seasonally wet and dry soils (Brinkman, 1970). The less soluble elements like aluminium and silicon remain in the soil and rock profiles in much higher concentrations and are moved out of the system by dissociation at much slower rates than the other chemical constituents. However, research has

shown that clay minerals such as kaolinite and montmorillonite (which are both rich in aluminium and silicon) will naturally weather in acidic conditions during the process of ferrolysis – especially in the presence of a fluctuating water table (Brinkman, 1970; Brinkman, 1979).

The relationship between silicon and iron is of particular interest in this instance as most of the silicon in Shadow Vlei exists as quartz which is highly resistant to weathering and it is unlikely that it will be removed from the soil profile. However, SiO_2 concentrations in Shadow Vlei vary from 55 % to 97 % which means that the concentration of SiO_2 is being affected by the movement of other ions. For a given SiO_2 concentration, Fe_2O_3 concentration is low in the central or internal areas of the depression (Figure 19), which is indicative of loss of iron in the iron reduction phase of ferrolysis. In contrast, for a given SiO_2 concentration, Fe_2O_3 concentration is high in the samples collected from the wetland margins, which is indicative of iron enrichment in the oxidation phase of ferrolysis where iron precipitates from solution as an iron oxyhydroxide. Iron precipitation may either dilute the SiO_2 concentration in a way that is reflected in geochemical mixing models, or it may involve substitution of silica by iron.

It is possible that substitution and dilution of SiO_2 occur simultaneously in the depression margin if, for example, for every two iron ions entering the depression margin, only one silicon ion is displaced from this zone. Enrichment of silicon occurs either when silicon is being deposited in an area or when other ions are being removed from an area and the relative concentration of SiO_2 therefore increases.

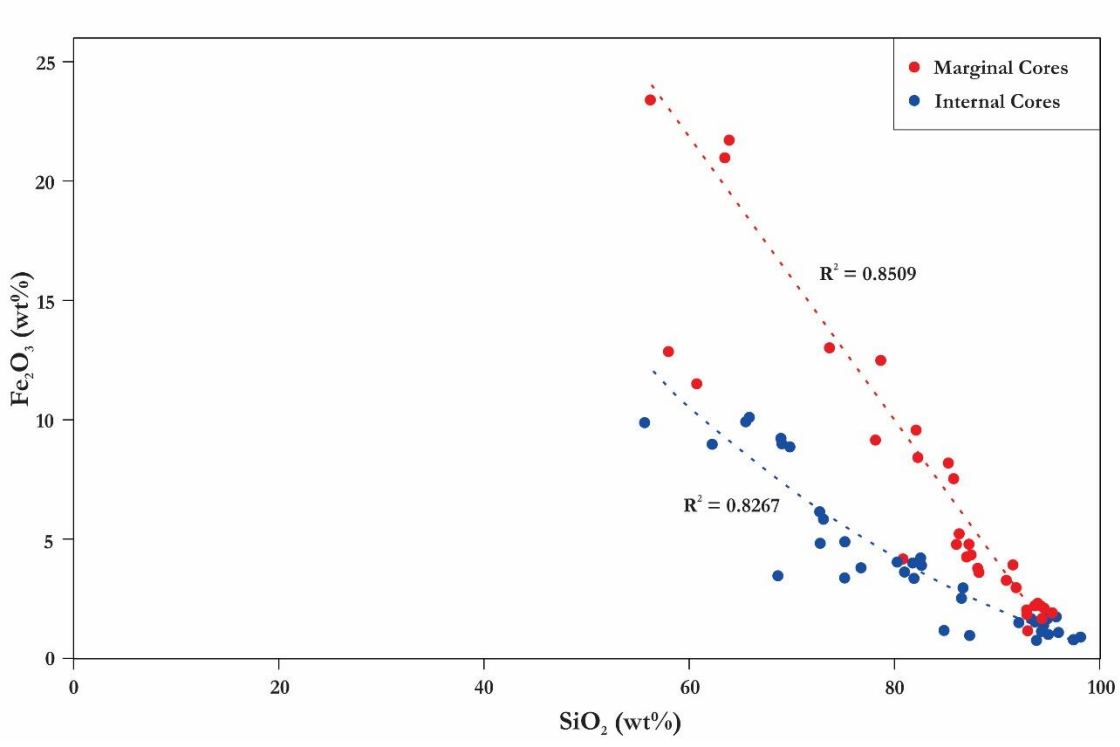

Figure 19: Relationships between Fe_2O_3 and SiO_2 concentration for samples taken from the depression margin and from the central part of Shadow Vlei.

7.5.1 Factors related to the perched water table of Shadow Vlei

The role that a perched water table has played in the formation of Shadow Vlei is important to consider in the climatic context of the Nelson Mandela Bay Municipality (NMBM). The widespread distribution of wetlands in the NMBM is unusual given the fact that wetland formation and preservation require a water-balance where inflows of water are greater than outflows, such that there is a positive water balance for a lengthy period (>1 month of continuous flooding) during the year. However, in the NMBM, the mean annual evaporation is as much as three times the MAP, such that a negative water-balance is a prominent feature of wetlands in NMBM (Melly *et al.,* 2017). These wetlands rely very little on sub-surface water inputs and most of the wetlands documented by Melly *et al.* (2017) and Schael *et al.* (2015) are precipitation-fed depression wetlands. Melly *et al.* (2017) investigated the presence of perched water tables in 46 depression wetlands and confirmed the presence of perched water tables in 34 of these wetlands. Most perches in wetlands in NMBM exist within the top 2 m of the soil profile and therefore have a near immediate effect on limiting infiltration of rainfall into the ground-water. The presence of a perched water table in a depression wetland sustains a prolonged period of inundation as the vertical infiltration and movement of water is reduced and slow lateral movement of ground water predominates. Perched water tables are often associated with layers of clay, quartz, calcrete, silcrete or ferricrete, as these minerals and duricrusts can form semi-impermeable layers that hinder vertical flow of water below ground (Dippenaar, 2014).

The presence of clay minerals in Shadow Vlei was confirmed in this study as both kaolinite and montmorillonite clays were detected. The highest concentrations and occurrence of these clay minerals were found in the centre of the depression, which supports the inference of a perched water table. However, the clay minerals are relatively depleted in the margins of the wetland where the majority of the ferricrete is located. The occurrence of these perches plays an integral part in the formation of wetlands in NMBM and it is important to try and understand their origin.

7.6 Conceptual model for the formation of Shadow Vlei

In the early stages, Shadow Vlei was a small, naturally occurring depression that, once filled, held and retained water for prolonged periods of time. The cycling between wet and dry periods in the

depression led to the alternation between anaerobic and aerobic conditions (Figure 20A and 20B). During the waterlogged phase of this cycle, anaerobic conditions were created which led to the reduction of ferric iron located below the depression by soil microbes. This reduction in the depression resulted in the breakdown of ferric iron minerals to form ferrous iron in solution. Due to the lateral movement of groundwater away from the depression centre, the ferrous iron would have been transported towards the margins of the depression. Once the water table started to drop and oxidising conditions were created, the ferrous iron in solution would have precipitated from solution as soon as it encountered an oxygen rich zone (Figure 20B). This draining of the soil profile and the creation of aerobic conditions led to the formation of acidity and ferric oxyhydroxides such as goethite. After many repetitions of this cycle, iron was slowly depleted from the centre of the depression and enriched in the margins, and in the case of Shadow Vlei, the formation of ferricrete in the margins accompanied this outward redistribution of iron. The formation of ferricrete in the margins of Shadow Vlei lead to some of the aggradation observed in these areas.

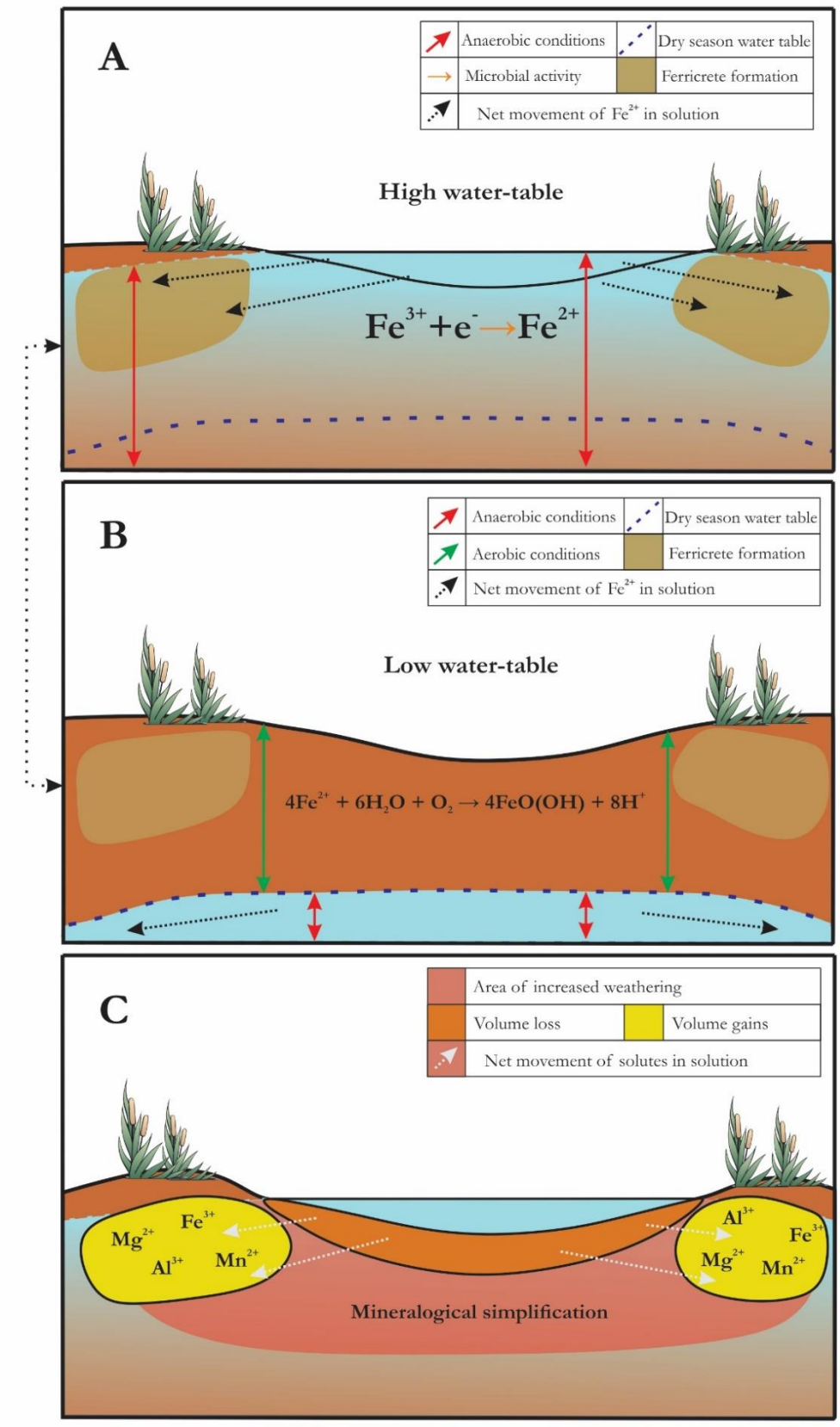

Figure 20: Conceptual model for the formation of Shadow Vlei. (A) Reducing phase of ferrolysis cycle during wet season (B) Oxidising phase of ferrolysis cycle during dry season (C) Aggradation and sagging processes responsible for formation of Shadow Vlei.

The iron-cycling process during ferrolysis will ultimately continue forever provided there is iron, both aerobic and anaerobic conditions in waterlogged soils and iron reducing soil microbes. Thus, Shadow Vlei is still currently expanding as the iron contained within it is continuously being cycled between its reduced and oxidised form and is gradually being moved farther away from the centre of the depression. However, due to conditions created both by the acidity produced during the oxidation of ferrous iron and the absence of oxygen, other minerals are chemically weathered in the centre of the depression as well. This process of weathering resulted in the mineralogical simplification of the material in the centre of Shadow Vlei and the lateral transport of dissolved solutes towards the margins of the wetland (Figure 20C). This mineralogical simplification was responsible for the formation of clay minerals below Shadow Vlei and the creation of a perched water table. Over time, mineralogical simplification caused the centre of Shadow Vlei to lose volume because of net solute removal, and the margins of the wetland to gain volume because of net solute accumulation. The movement of iron in the soil profile has occurred over several million years and has resulted in the gradual expansion of the depression over time (Figure 21). As the cycle of iron oxidation and reduction occurs in an ever-outward direction, more iron will become accessible for redistribution, hence the growth of the ferricrete outcrops in the margins over time. The constant migration of iron and other soluble elements towards the margins have ultimately resulted in the deepening and widening of the depression over time (Figure 21).

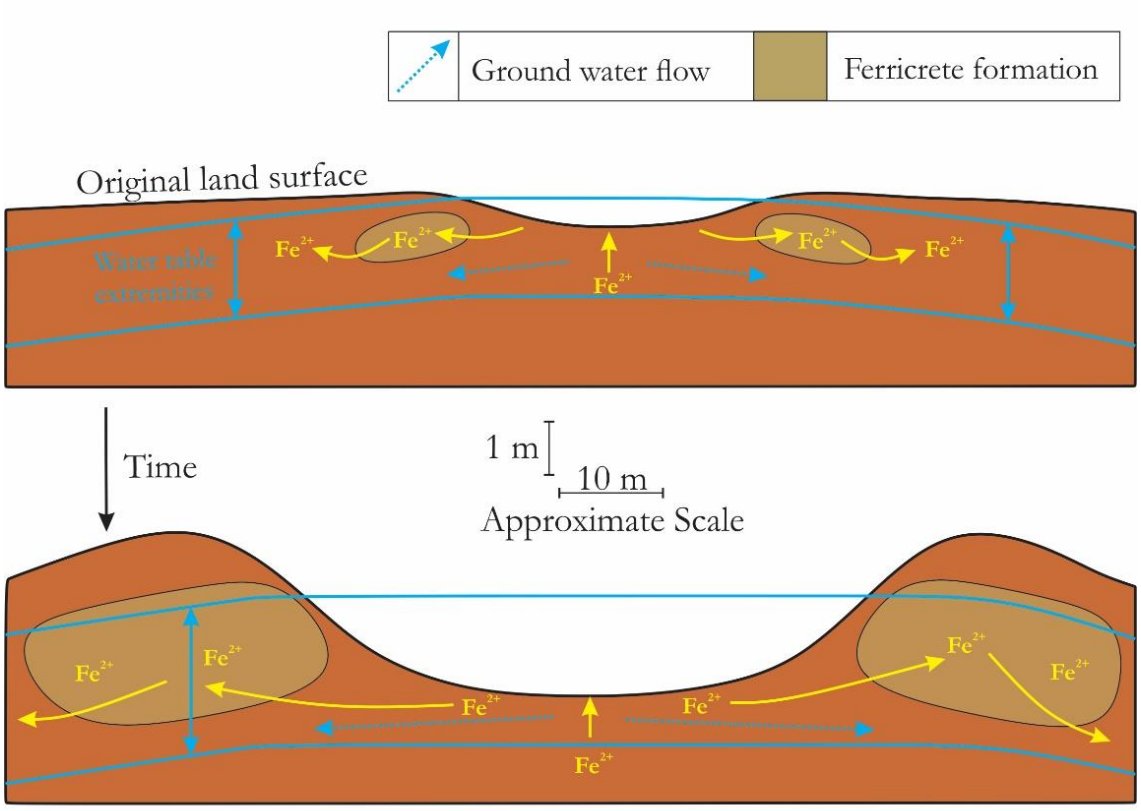

Figure 21: Conceptual model of the spatial evolution and progression of Shadow Vlei over time.

7.7 Is Shadow Vlei a unique feature?

The combination of processes that are presented in this study to lead to the formation of Shadow Vlei are novel as far as I am aware – but that does not mean that it is an anomalous or unique feature in the landscape. The model of depression wetland formation proposed by Thomas and Goudie (1985) has been the ubiquitous explanation for the occurrence of depression wetlands in arid and semi-arid areas for many years, but does not effectively explain the formation of Shadow Vlei, nor does it explain the formation of Dartmoor Vlei studies by Edwards *et al.* (2016) or the depression wetland studied by Alistoun (2014). However, the processes of wetland formation described in Edwards *et al.* (2016) and by Alistoun (2014) do not explain the formation of Shadow Vlei either.

The progression of wetland formation described in Edwards *et al.* (2016) is different from that in Shadow Vlei as Dartmoor Vlei was formed primarily through the process of sagging and mineralogical simplification. It was calculated that the original land surface in Dartmoor Vlei has been lowered by an average of 8.4% (just over 1 m) across the wetland surface – which is a significant amount considering that the wetland is 42 ha in size. This kind of volume loss would

only be observed as a result of significant mineralogical simplification via the weathering of a complex parent material. Dartmoor Vlei is situated on dolerite which has many weatherable constituents in it such as anorthite ($\overline{x}$ = 31.36%), albite ($\overline{x}$ = 28.13%), wollastonite ($\overline{x}$ = 14.9%), quartz ($\overline{x}$ = 8.1%), enstatite ($\overline{x}$ = 8.03%) and orthoclase ($\overline{x}$ = 4.94%) (Edwards *et al.,* 2016). Many of these mineralogical constituents are easily weathered in the presence of water. In contrast, the mineralogy of Shadow Vlei is primarily comprised of quartz, a limited number of clay minerals and goethite – all of which are resistant to chemical weathering. Therefore, the extent of sagging that has occurred in Dartmoor Vlei is much greater than that which has occurred in Shadow Vlei.

Shadow Vlei differs from the depression wetland studied by Alistoun (2014) for this reason as well – as dwyka tillite also has a much more complex mineralogy than the Table Mountain Group Sandstone upon which Shadow Vlei sits. This means that the volume loss in the centre of the wetland north of Grahamstown would have been greater on dwyka tillite than in Shadow Vlei. The process of aggradation in Shadow Vlei is explained by a completely different process to the wetland studied by Alistoun (2014). Selective uptake of solutes by deep-rooted trees in the margins of the Grahamstown wetland is primarily responsible for the concentration and precipitation of solutes in the margins of the wetland. In Shadow Vlei, aggradation at the margins of the wetland can be accounted for by ferrolysis and the formation of ferricrete, and primarily involves the redistribution of iron in the soil profile. The process of soil chloritisation could be a mechanism that is concentrating solutes in the margins of the wetland studied by Alistoun (2014), but further investigation would be required to confirm this. The process that leads to the formation of depressions on islands in the Okavango Delta can also be included in this comparison as it occurs primarily through a process of aggradation as a result of selective uptake of solutes by trees growing on the margins of the islands – much like the aggradation described by Alistoun (2014). However, no sagging of the land surface takes place in the process of island formation in the Okavango Delta and this can be attributed to the fact that the bedrock upon which the delta sits is a quartz-rich sandstone. Most solutes that are trapped in the Okavango islands come from the catchment of the delta due to weathering of a region of the catchment of granite, which weathers to produce solutes such as Ca, Mg, Na and K which make up the majority of the precipitates in the islands in the Okavango (Ellery *et al.,* 1993).

7.8 Incorporating geomorphology into models of wetland structure and function

The origin, structure and function of Shadow Vlei is clearly linked to geomorphic processes that occur over prolonged periods of time. Thus, the importance of geomorphology in shaping the hydrological, edaphic and biotic regimes in Shadow Vlei cannot be overlooked. The evidence presented in this thesis points to the long-term co-evolution and development of geomorphic and hydrological processes that have resulted in the formation of Shadow Vlei and the edaphic and biotic processes that characterise the wetland. The role that geomorphology plays in the origin and evolution of wetlands in general is often poorly understood and this can lead to poor conservation, management and restoration practices that are advocated both by wetland scientists and managers (Tooth and McCarthy, 2007). The currently accepted model of wetland structure and function proposed by Mitsch and Gosselink (2015) describes geomorphology as a template upon which hydrological and physiochemical processes act together to create conditions conducive to wetland formation. However, the insight that the Mitsch and Gosselink (2015) model provides into explaining wetland structure and function is limited, and as water resources become scarce and increasingly valuable, a deeper, more holistic understanding of wetlands is necessary for conservationists and managers. Thus, a new conceptual model that considers lithology, climate, landscape form and hydrology as active controls of the origin, structure, function and dynamics of wetlands is proposed in Figure 22. The interaction of the geomorphic processes of a wetland (depicted in the brown box) will have a major influence on the wetland's ecological processes (depicted in the green box) and will ultimately determine the form and dynamics of a wetland system. The geomorphic processes in Figure 22 typically occur over a longer temporal scale than the ecological processes, and are often working, unseen, before ecological processes characteristic of wetland structure and function are observed.

The formative phase of a wetland and its resultant structure is a direct consequence of both lithological and climatic controls as these will affect both the landscape form and the hydrological regime. For example, the lithology and climate have played an integral role in the formation of Shadow Vlei as its formation can only be explained in the context of a sufficiently iron-rich parent material and a climate that allows for alternating periods of soil water-logging and desiccation. Had the lithology been a highly metamorphosed iron-poor quartzite, Shadow Vlei would not exist in its current form and it is likely that it may not have existed at all. The lithology and the structural/tectonic history of a wetland site also has a direct impact on the topography and morphology of the initial landscape, which in the case of the system being considered was gently

undulating to flat, which meant that localised ponding was possible. Climate affects both the landscape form and the hydrological regime as it affects phenomena such as the depth of weathering, likelihood of erosion and biotic interactions with the landscape (Figure 22). The interaction between landscape form and hydrological regime is significant: in the context of Shadow Vlei, shallow ponding and isolation of the land surface from the larger fluvial system initially led to the initiation of ferrolysis on a local scale. An understanding of how surface and near-surface water interacts with the pre-existing landform is required to explain the current form of Shadow Vlei. The origin, formation, structure and functioning of Shadow Vlei cannot be unpacked looking solely at the hydrological, physiochemical and biotic factors, as is suggested in Mitsch and Gosselink's (2015) wetland model.

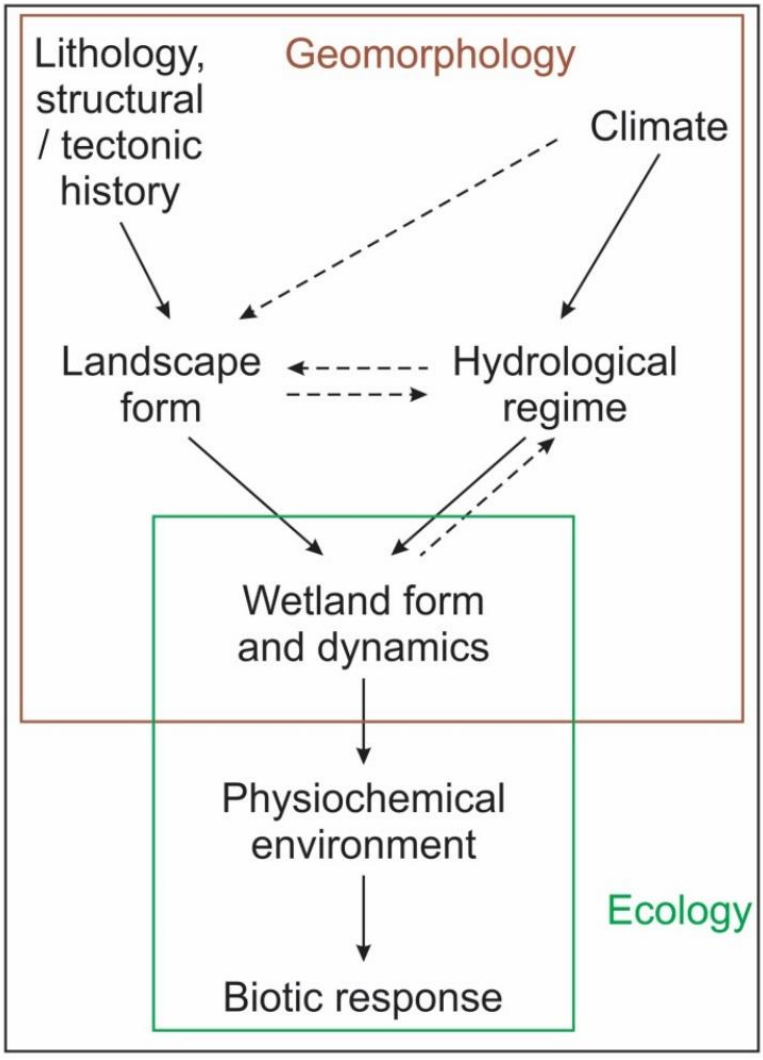

Figure 22: Conceptual model illustrating the fundamental role of geomorphology in the structure and function of wetland systems.

The relationship between landscape form and hydrological regime has been unpacked before in various contexts such as; Nylsvlei and Wakkerstroom Vlei, where tributary alluvial fan floodouts block a trunk stream, leading to the formation of an unchanneled valley-bottom wetland (McCarthy *et al.*, 2011; Joubert and Ellery, 2013). The Futululu and Mdlanzi unchanneled valley-bottom wetlands were formed where trunk stream alluvial ridge accretion have blocked tributaries (Grenfell *et al.,* 2008; Grenfell *et al.*, 2010), but the importance of understanding this relationship has been understated in most of these papers.

The study of Tooth *et al.* (2002) illustrates that the hydrological regime is the main driver of wetland formation and change, but also how the hydrology is fundamentally guided by geomorphic processes (Figure 23). Tooth *et al.* (2002) studied the formation of alluvial meanders and floodplain wetlands on the Klip River in the eastern Free State, where easily weathered and eroded Karoo sediments are extensively intruded by dolerite dykes. As the Klip River eroded its bed into Karoo sediments, a buried dolerite dyke oriented across the valley was exposed (Figure 23). Since dolerite is very resistant to weathering and erosion, it forms a local base level and the incision of the bed of the Klip River was therefore unable to incise Karoo sediments at a faster rate than the rate at which the dolerite dyke could be eroded. At this point the Klip River would have eroded its bed upstream of the dolerite dyke to an appropriate gradient for the available discharge, after which it would have started to meander and plane the valley laterally such that a floodplain wetland was formed (Tooth *et al.*, 2002). In this context, the hydrological regime and the movement of water across the landscape was the driving force behind valley incision and valley widening, which were responsible for the formation of this remarkable high-altitude floodplain. It is not possible to fully explain and understand wetland form and dynamics in the Klip River simply by considering the hydrological, physiochemical and biotic components of this floodplain wetland, but the understanding generated by incorporating geomorphic processes is significant.

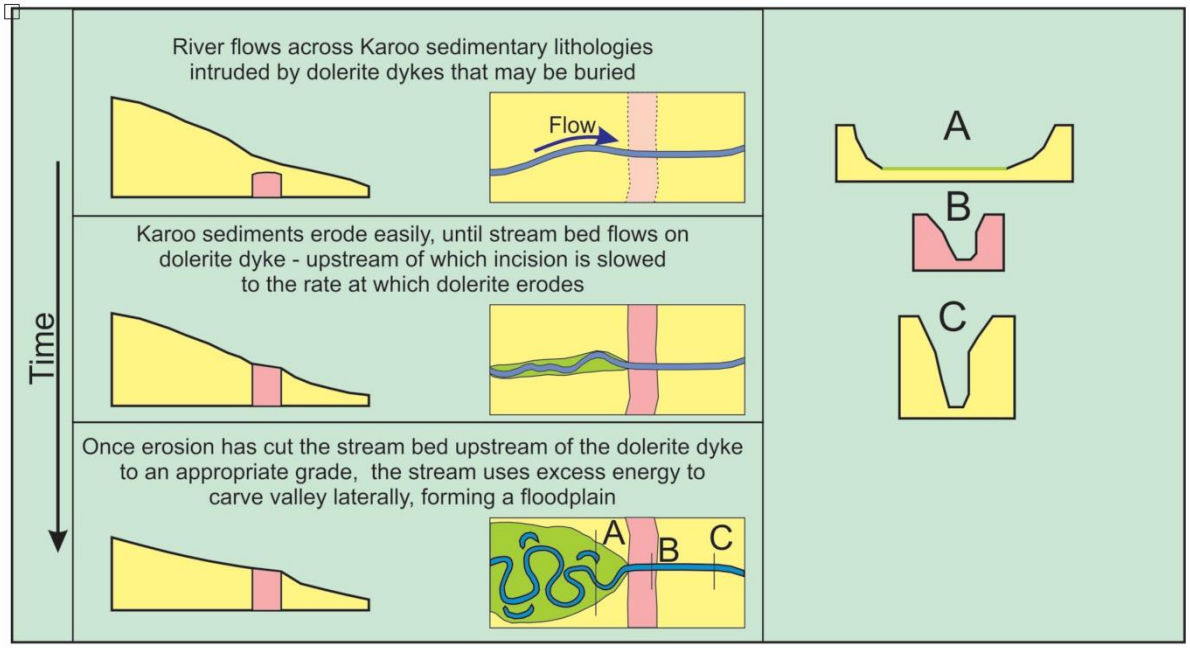

Figure 23: Conceptual model illustrating the formation of meandering alluvial streams and a floodplain wetland in the Klip River, South Africa (adapted from Tooth *et al.,* 2002).

The importance of this understanding for wetland management is vital. For instance, a hallmark of meandering floodplain wetlands is the formation of an alluvial ridge due to deposition of fine sediment as overbank deposits during flood events. Aggradation of the alluvial ridge over time inevitably results in channel avulsion, which may or may not be accelerated by human activities. Wetland managers are generally of the view that radical changes in flow such as those associated with channel avulsion, are disastrous events and need rectification. Such a case study is presented by Ellery *et al.* (2003) for the Mkuze River, where a minor manual excavation from the Mkuze River to the backswamp led to the diversion of the course of the river along a watercourse through former backswamp. The landowner responsible was charged and sentenced to reinstating the flow of water along the former course of the Mkuze River. The study by Ellery *et al.* (2003) revealed that the diversion simply accelerated a natural avulsion, and that there was a remote prospect of ever diverting flow back down along the former course of the Mkuze River. This case study highlights the importance of understanding the geomorphology of a wetland and how poor knowledge of geomorphic processes can have disastrous and costly effects.

8 Conclusion

The origin of Shadow Vlei is inherently linked to geomorphic processes that only occur over prolonged periods of time and can only be observed and measured in hindsight as they are extremely slow acting. Processes of iron-cycling and chemical weathering are responsible for the formation of the morphology of Shadow Vlei which in turn have influenced the soil and vegetation structure in the wetland. The presence of a perched water table also influences the soils and vegetation in the depression. The perch contributes both to the constant presence of vegetation in the depression as well as to the cycling of iron below the surface. Interactions between geomorphic and hydrological processes in Shadow Vlei are fundamentally linked and act together to produce the wetland form and dynamics.

8.1 Revision of objectives

It is important to reflect on the initial aim and objectives of a thesis to assess the relative success of the study as well as the relative confidence that can be attached to the arguments that have been presented. The overarching aim of the study was to determine the geomorphic processes responsible for the formation of Shadow Vlei. This aim was achieved to the desired extent, although it wasn't necessarily achieved through completing the objectives set out at the beginning of the study.

8.1.1 Objective 1: Mapping geochemistry and mineralogy

The objective of accurately mapping spatial variation in geochemistry and mineralogy with depth and across the length and breadth of Shadow Vlei was partially achieved. Variation in the distribution of major elements was completed and well understood. The processes that drive this variation in the chemistry vertically and horizontally were also well understood and can be explained by the redistribution of iron and other elements as a result of weathering, redox reactions and groundwater recharge flows. Understanding of the geochemistry of Shadow Vlei is better than of the mineralogy as a consequence of the difficulties that were encountered with quantitative XRD analysis. However, the geochemistry was used to inform the mineralogy, and this resulted in a relatively accurate and reliable understanding of the distribution of minerals below the depression. The mineralogical variation in Shadow Vlei can be explained by similar processes as the variation in the geochemistry.

8.1.2 Objectives 2 and 3: Mapping topography and linking topography to geochemistry and mineralogy

The topography of Shadow Vlei was effectively and accurately mapped in relation to the surrounding land surface. The geochemistry was successfully mapped in relation to the topography and it was through this mapping and untangling of the geochemical data in relation to the topography that iron-cycling was proposed as a geomorphic process that is ongoing and responsible for the formation of ferricrete and elevated depression margins. Loss of solutes from the soil beneath the centre of the depression is considered to contribute to sagging. In contrast to the chemistry, the mineralogy was less successfully tied to the topography of the depression as there were fewer samples that had mineralogical data and therefore the resolution of the mineralogical data was much coarser. However, the combination of the geochemical data and the mineralogy allowed for a more confident reflection on the geomorphic processes responsible for the formation of Shadow Vlei.

8.1.3 Objective 4: Determining interactions between surface water and ground water

The relationship between the surface and the ground water table could not be analysed in this study as the Eastern Cape has been experiencing an extreme drought and there was no water on the surface or below ground to the depths at which coring was undertaken. However, evidence of a perched water table was observed both in this study and in Melly *et al.* (2017) which gave an indication to a relationship that would typically exist between surface water and a perched ground water table. Using evidence presented in peer reviewed articles and postgraduate theses, an understanding of the surface water - ground water interaction is confidently presented.

8.1.4 Objective 5: Conceptual model for origin and evolution of Shadow Vlei

Based on the evidence collected throughout this study, the conceptual model of the origin and evolution of Shadow Vlei were formulated and presented. As far as I am aware, the conceptual model presented here is novel and can be integrated into the growing suite of wetland depression origin models that are characterised by geomorphic processes.

8.2 Future research

The insight that has been gained throughout this study has led to the formulation of many more questions and potential areas for future research. Shadow Vlei is a perfect example of a closed

iron-cycling system that could be studied further for insights into how this process is linked to geomorphic evolution of such wetlands. Iron-cycling has been documented in many parts of the world but is often studied in the context of soil formation and the morphologic effect that iron-cycling has generally been understated and poorly appreciated. The redistribution of iron as a result of a fluctuating water table can clearly have a large effect on the morphology of a landscape, and this process should be recognised as contributing to wetland formation. Therefore, it is important that the process of iron cycling is documented in other wetland contexts such that a growing understanding of these systems can be created.

A part of the iron-cycling process that was poorly understood in this study was the role that soil microbes, particularly iron-reducing bacteria, play in the reduction and redistribution of iron. A study of the soil bacteria that exist in Shadow Vlei might contribute to understanding the process of iron-cycling and ferrolysis. It may also be that the microbial flora of these pans is unique given that so little work of this kind has been undertaken in southern Africa.

Finally, broader research should be conducted on the role that geomorphology plays in the structure and function of wetlands. Integration of geomorphology into Mitsch and Gosselink's (2015) model of wetland structure and function needs to be supported by wider research and documentation of geomorphic and geochemical processes that lead to the formation, structure and functioning of wetlands. As water resources become increasingly limited and scarce, deeper understanding of how hydrological systems operate to create wetlands and influence their dynamics is required, such that the impacts of altered hydrological regimes on wetlands can be predicted. It is our responsibility as the main agents of wetland modification and destruction to better understand how they work and how we can make better, more informed decisions around their management and conservation. It is important as a community of practice, that wetland scientists are able to leave their egos outside of the discussions held around wetland structure and function, and that we strive to do what is best for the systems that we are damaging.

9 Reference List

Alistoun, J. 2014. *The origin of endorheic pans on the African Erosion Surface north of Grahamstown, South Africa*. Grahamstown: Rhodes University (MSc Dissertation) [PDF].

Ambrosi, J.P., Nahon, D. and Herbillon, A.J. 1986. The epigenetic replacement of kaolinite by hematite in laterite - petrographic evidence and the mechanisms involved. *Geoderma*, 37(4), 283–294.

Anderson, R.S. and Anderson, S.P. 2010. *Geomorphology: the mechanics and chemistry of landscapes* (3e). Cambridge: Cambridge University Press.

Birkeland, P.W. 1984. *Soils and Geomorphology* (1e). Oxford: Oxford University Press.

Bish, D.L. and Howard, S.A. 1988. Quantitative phase analysis using the Rietveld method. *Journal of Applied Crystallography*, 21(2), 86–91.

Bowen, M.W., Johnson, W.C., Egbert, S.L. and Klopfenstein, S.T. 2010. A GIS-based approach to identify and map playa wetlands on the High Plains, Kansas, USA. *Wetlands*, 30(4), 675–684.

Bridge, T.A. and Johnson, D.B. 1998. Reduction of soluble iron and reductive dissolution of ferric iron-containing minerals by moderately thermophilic iron-oxidizing bacteria. *Applied and environmental microbiology*, 64(6), 2181–2186.

Brinkman, R. 1970. Ferrolysis, a hydromorphic soil forming process. *Geoderma*, 3(3), 199–206.

Brinkman, R. 1979. *Ferrolysis, a soil-forming process in hydromorphic conditions*. Wageningen: Landbouwhogeschool van Wageningen (PhD Dissertation) [PDF].

Butt, C.R.M. and Bristow, A.P.J. 2013. Relief inversion in the geomorphological evolution of sub-Saharan West Africa. *Geomorphology*, 185(1), 16–26.

Conacher, A.J., Ollier, C.D. and Galloway, R.W. 1991. Lateritic duricrust and relief inversion in Australia. *Catena*, 18(1), 585–588.

Cousins, J.A., Sadler, J.P. and Evans, J. 2008. Exploring the role of private wildlife ranching as a conservation tool in South Africa: Stakeholder perspectives. *Ecology and Society*, 13(2) 56-71.

Cowling, R.M. 1983. Diversity relations in Cape shrublands and other vegetation in the southeastern Cape, South Africa. *Vegetation*, 54(2), 103–127.

Detenbeck, N.E. 2002. Methods for Evaluating Wetland Condition #7: Wetlands Classification. *United States Environmental Protection Agency, Office of Water,* March 2002(1), 43-88.

Dippenaar, M.A. 2014. Towards hydrological and geochemical understanding of an ephemeral palustrine perched water table "wetland"(Lanseria Gneiss, Midrand, South Africa). *Environmental earth sciences*, 72(7), 2447–2456.

Dugan, P. 1993. *Wetlands in danger: a world conservation atlas*. (1e). New York: Oxford University Press.

Dunlevey, J. 2018. Professor, University of Limpopo. Personal Communication. 27 January.

Edwards, R.J., Ellery, W.N. and Dunlevey, J. 2016. The role of the in situ weathering of dolerite on the formation of a peatland: The origin and evolution of Dartmoor Vlei in the KwaZulu-Natal Midlands, South Africa. *Catena,* 143(2), 232–243.

Ellery, W.N., Ellery, K. and McCarthy, T.S. 1993. Plant distribution in islands of the Okavango Delta, Botswana: determinants and feedback interactions. *African Journal of Ecology*, 31(2), 118–134.

Ellery, W.N., McCarthy, T.S. and Dangerfield, J.M. 1998. Biotic factors in mima mound development: evidence from the floodplains of the Okavango Delta, Botswana. *International Journal of Ecology and Environmental Sciences*, 24, 293–313.

Ellery, W.N., Dahlberg, A.C., Strydom, R., Neal, M.J. and Jackson, J. 2003. Diversion of water flow from a floodplain wetland stream: an analysis of geomorphological setting and hydrological and ecological consequences. *Journal of Environmental Management*, 68(1), 51–71.

Ellery, W.N., Grenfell, M.C., Grenfell, S.E., Kotze, D., McCarthy, T.S., Tooth, S., Grundling, P.L., Beckendahl, H., Le Maitre, D. and Ramsay, L. 2011. WET-origins: controls on the distribution and dynamics of wetlands in South Africa. *WRC Report*, 334(9).

Fey, M. 2010. *Soils of South Africa* (1e). Cape Town: Cambridge University Press.

Fitzpatrick, R.W. and Schwertmann, U. 1982. Al-substituted goethite-An indicator of pedogenic and other weathering environments in South Africa. *Geoderma*, 27(4), 335–347.

Goudie, A.S. and Thomas, D.S.G. 1985. Pans in southern Africa with particular reference to South Africa and Zimbabwe. *Zeitschrift fur Geomophologie*, 29(1), 1–19.

Grenfell, M.C., Ellery, W.N. and Grenfell, S.E. 2008. Tributary valley impoundment by trunk river floodplain development: a case study from the KwaZulu-Natal Drakensberg foothills, eastern South Africa. *Earth Surface Processes and Landforms*, 33(13), 2029–2044.

Grenfell, S.E., Ellery, W.N. and Grenfell, M.C. 2009. Geomorphology and dynamics of the Mfolozi River floodplain, KwaZulu-Natal, South Africa. *Geomorphology*. 107(3–4), 226–240.

Grenfell, S.E., Ellery, W.N., Grenfell, M.C., Ramsay, L.F. and Fluegel, T.J. 2010. Sedimentary facies and geomorphic evolution of a blocked-valley lake: Lake Futululu, northern Kwazulu-Natal, South Africa. *Sedimentology*, 57(5), 1159–1174.

Jacobs, T.L. 2017. *A meterological analysis of extreme flood events in the southern parts of the Eastern Cape, South Africa*. Grahamstown: Rhodes University (MSc Dissertation) [PDF].

Johnson, D.B. and McGinness, S. 1991. Ferric Iron Reduction by Acidophilic Heterotrophic Bacteria. *Applied Environmental Microbiology*, 57(1), 207–211.

Joubert, R. and Ellery, W.N. 2013. Controls on the formation of Wakkerstroom Vlei, Mpumalanga province, South Africa. *African Journal of Aquatic Science*, 38(2), 135–151.

Krzic, M. 2004. *SoilWeb200: An online teaching tool for APBI 200 course*, *University of Bristish Colombia*. [Online].
http://soilweb200.landfood.ubc.ca/soil-components/1-mineral-components/#Weathering.
[23/04/2017].

Lee, S.Y. and Gilkes, R.J. 2005. Groundwater geochemistry and composition of hardpans in southwestern Australian regolith. *Geoderma*, 126(1–2), 59–84.

Luther, G.W., Kostka, J.E. and Church, T.M. 1992. Seasonal iron cycling in the salt-marsh sedimentary environment : the importance of ligand complexes with Fe (II) and Fe (III) in the dissolution of Fe (III) minerals and pyrite , respectively. *Marine chemistry,* 40(1-2), 81–103.

Macvicar, C.N. and Soil Classification Working Group. 1991. *Soil classification: A taxonomic system for South Africa* (2e). Pretoria: Department of Agricultural Development.

Mann, A.W. 1983 Hydrogeochemistry and weathering on the Yilgarn Block, Western Australia-ferrolysis and heavy metals in continental brines. *Geochimica et Cosmochimica Acta*, 47(2), 181–190.

Maud, R.R. 2008 The Macro-Geomorphology of the Eastern Cape. *In* Lewis, C.A. (eds), *Geomorphology of the Eastern Cape* (2e). Grahamstown: NISC, pp. 1–20.

Mcbride, E.F. 1963. A classification of common sandstones. *Journal of Sedimentary Research*, 33(3), 664-669.

McCarthy, T.S., Ellery, W.N. and Ellery, K. 1993. Vegetation-induced, subsurface precipitation of carbonate as an aggradational process in the permanent swamps of the Okavango (delta) fan, Botswana. *Chemical Geology*, 107(1–2), 111–131.

McCarthy, T.S. and Ellery, W.N. 1994. The effect of vegetation on soil and ground water chemistry and hydrology of islands in the seasonal swamps of the Okavango Fan, Botswana. *Journal of Hydrology*, 154(1–4), 169–193.

McCarthy, T.S. and Ellery, W.N. 1998. The okavango delta. *Transactions of the Royal Society of South Africa*, 53(2), 157–182.

McCarthy, T. S. and Hancox, P. J. 2000. Wetlands. *In* Partridge, T.C. and Maud, R.R. (eds), *The Cenozoic of Southern Africa*. Oxford: Oxford University Press, 56-89.

McCarthy, T. S., Rowberry, M.D., Brandt, D., Hancox, P.J., Marren, P.M., Tooth, S., Jacobs, Z., Thompson, M., Woodborne, S. and Ellery, W.N. 2011. The origin and development of the Nyl river floodplain wetland, limpopo province, South Africa: Trunk-tributary river interactions in a dryland setting. *South African Geographical Journal*, 93(2), 172–190.

McQueen, K.G. 2005. Towards understanding the ferruginous component of the regolith. *In* Anand, R.R. and Morris, P. (eds), *Minerals Exploration Seminar*. Kalgoorlie: Cooperative Research Centre for Landscape Environments and Mineral Exploration, 18.

Melly, B.L., Schael, D.M. and Gama, P.T. 2017. Perched wetlands: An explanation to wetland formation in semi-arid areas. *Journal of Arid Environments*, 141, 34–39.

Midgeley, D.C., Pitman, W.V. and Middleton, B.J. 1994. *Surface Water Resources of South Africa*. Pretoria: Water Research Commission.

Millot, G. 2013. *Geology of Clays: Weathering, Sedimentology,·Geochemistry*. Berlin: Springer Science & Business Media.

Mitsch, W.J. and Gosselink, J.G. 2015. *Wetlands* (5e). New York: John Wiley & Sons.

Mucina, L. and Rutherford, M.C. 2006. *The vegetation of South Africa, Lesotho and Swaziland*. Pretoria: South African National Biodiversity Institute.

O'Connor, T.G. and Crow, V.R.T. 1999. Rate and pattern of bush encroachment in Eastern Cape savanna and grassland. *African Journal of Range and Forage Science*, 16(1), 26–31.

Pain, C.F. and Ollier, C.D. 1992. Ferricrete in Cape York Peninsula, north Queensland. *BMR Journal of Australian Geology & Geophysics*, 13(3), 207–212.

Partridge, T.C. and Maud, R.R. 1987. Ceomorphic evolution of southern Africa since the Mesozoic. *South African Journal of Geology*, 90(2), 179–208.

Phillips, J.D., Lampe, M., King, R.T., Cedillo, M., Beachley, R. and Grantham, C. 1997. Ferricrete formation in the North Carolina coastal plain. *Zeitschrift fur Geomophologie*, 41(1), 67–80.

Phillips, J.D. 2000. Rapid development of ferricretes on a subtropical valley side slope. *Geografiska Annaler. Series A: Physical Geography*, 82(1), 69–78.

Reddy, K.R. and D'Angelo, E.M. 1997. Biogeochemical indicators to evaluate pollutant removal efficiency in constructed wetlands. *Water Science and Technology*, 35(5), 1–10.

Schael, D.M., Gama, P.T. and Melley, B.L. 2015. *Ephemeral Wetlands of the Nelson Mandela Bay Metropolitan Area : Classification , Biodiversity and Management Implications*. [Online] Pretoria: Water Research Comission. Available at: doi: 10.13140/RG.2.1.2029.9122 [27/12/2017]

Schwarz, T. 1994. Ferricrete formation and relief inversion: an example from Central Sudan. *Catena*, 21(2–3), 257–268.

Schwertmann, U. 1991 Solubility and dissolution of iron-oxides. *Plant Soil*, 130, 1–25.

Sinchembe, M. and Ellery, W.N. 2010. Human impacts on hydrological health and the provision of ecosystem services: A case study of the eMthonjeni-Fairview Spring Wetland, Grahamstown, South Africa. *African Journal of Aquatic Science*, 35(3), 227–239.

Singleton, A.T. and Reason, C.J.C. 2007. A numerical model study of an intense cutoff low pressure system over South Africa. *Monthly weather review*, 135(3), 1128–1150.

Smith, P. A. 1976. An outline of the vegetation of the Okavango drainage system. in *Symposium on the Okavango Delta*. Gabarone: Botswana Society.

Taylor, G. and Eggleton, R.A. 2001. *Relogith geology and geomorphology*. West Sussex: John Wiley & Sons.

Thomas, D.S.G. 2011. Arid environments: their nature and extent. in Thomas, D.S.G. (eds) *Arid zone geomorphology: process, form and change in drylands* (3e.). New York: John Wiley & Sons, 1–16.

Tooth, S., McCarthy, T.S., Brandt, D., Hancox, P.J. and Morris, R. 2002. Geological controls on the formation of alluvial meanders and floodplain wetlands: The example of the Klip River, eastern Free State, South Africa. *Earth Surface Processes and Landforms*, 27(8), 797–815.

Tooth, S. and McCarthy, T.S. 2007. Wetlands in drylands: Geomorphological and sedimentological characteristics, with emphasis on examples from southern Africa. *Progress in Physical Geography*, 31(1), 3–41.

Towe, K.M. 1974. Quantitative clay petrology: The trees but not the forest? *Clays and Clay Minerals*, 22(5–6), 375–378.

Van Ranst, E. and De Coninck, F. 2002. Evaluation of ferrolysis in soil formation. *European Journal of Soil Science*, 53(4), 513–519.

Visser, J.N.J. 1974. The Table Mountain Group: a study in the deposition of quartz arenites on a stable shelf. *South African Journal of Geology*, 77(3), 229–237.

Weber, K.A., Achenbach, L.A. and Coates, J.D. 2006. Microorganisms pumping iron : Anaerobic microbial iron oxidation and reduction. *Nature reviews micorbiology,* 4(10), 752-764.

White, A.F. and Brantley, S.L. 1995. Chemical weathering rates of silicate minerals; an overview. *Reviews in Mineralogy*, 31(1), 1–22.

Widdowson, M. 2003. Ferricrete. *In* Goudie, A.S. (eds) *Encyclopedia of Geomorphology* (1e). London: Routledge, 365–367.

Widdowson, M. 2007. Laterite and Ferricrete. *In* Nash, D.J. and McLaren, S J. (eds) *Geochemical Sediments & Landscapes* (1e). Singapore: Blackwell Publishing Ltd, 46–95.